Integrated, Regional-Scale Hydrologic Modeling of Inland Lakes

*Zachary J. Hanson, Jacob A. Zwart, Joseph Vanderwall, Christopher T. Solomon,
Stuart E. Jones, Alan F. Hamlet, and Diogo Bolster*

Research Impact Statement: This new modeling approach captures unique features of thousands of lakes in a region and enables predictions on the effects of land use and climate change on these important freshwater resources.

ABSTRACT: Inland lakes constitute an important global freshwater resource and are often defining features of local and regional landscapes. While coupled surface water (SW) and groundwater (GW) models are increasingly available, there is a clear need for spatially explicit yet computationally parsimonious modeling frameworks to explore the impacts of climate, land use, and other drivers on lake hydrologic and biogeochemical processes. To address this need, we developed a new method to simulate daily water budgets for many individual lakes at large spatial scales. By integrating SW, GW, and lake water budget models in a simple manner, we created a modeling framework capable of simulating the historical and future hydrologic dynamics of lakes with varying hydrologic characteristics. By extension, the model output enables ecological modeling in response to hydrologic drivers. As a case study, we applied the model to a large, lake-rich region in northern Wisconsin and Michigan, simulating daily water budgets for nearly 4,000 lakes over a 36-year period. Despite minimal calibration efforts, our simulated results compared reasonably well with observations and more sophisticated modeling approaches. Our integrated modeling requires very limited information, can be run on readily available computer resources, such as a desktop PC, and can be applied at regional, continental, or global scales, where necessary model setup and forcing data are available.

(KEYWORDS: surface water hydrology; groundwater hydrology; lakes; watersheds; simulation; aquatic ecology.)

INTRODUCTION AND BACKGROUND

Landscapes with high concentrations of inland lakes are often hydrologically interconnected due to interactions between surface water (SW) and groundwater (GW) (Winter 1999). Variations in hydrologic flowpaths (e.g., varying SW and GW fluxes for different lakes, or the presence or absence of streams) exert important controls on the spatial and temporal patterns of lake biogeochemical cycling (Vachon and del Giorgio 2014; Vachon et al. 2017; Zwart et al. 2017). These variations in hydrologic characteristics are driven by both local- and regional-scale processes. For example, physical and biogeochemical processes in lakes are directly affected by local-scale SW and GW fluxes, and human development. Over longer time scales, lakes are affected by changing climate and land use through regional-scale changes in temperature, precipitation, snow, catchment vegetation, and evapotranspiration. As knowledge of the hydrological and ecological importance of lakes continues

to grow, so too has the need to understand how the behavior of inland lakes will change in response to these drivers.

To fully understand the complex interactions between lakes and their catchments, integrated hydrologic models of coupled SW and GW processes, acting over a wide range of spatial scales, are needed. Typically, SW and GW models have been developed separately. The past several decades have seen the development and improvement of both independent SW models (Crawford and Linsley 1966; Feldman et al. 1981; Leavesley et al. 1983; Liang et al. 1994) and GW models alike (Trescott 1975; McDonald and Harbaugh 1984; Strack 1989; Torak 1993; Haitjema 1995; Harbaugh 2005). The interconnected nature of SW and GW resources has inspired research over the past decade in the development of several fully integrated surface and subsurface models (Bixio et al. 2002; Kollet and Maxwell 2006; Qu and Duffy 2007; Shen and Phanikumar 2010), and this field continues to grow. Such models incorporate complex feedbacks that play an important role in SW/GW interactions, but their use is currently constrained by significant data and computational costs. Many fully coupled models require detailed topography, soil, vegetation, and aquifer characteristics and must solve systems of highly nonlinear flow equations in order to describe multiphase flows through unsaturated and saturated soils. Numerical stability of such tools also requires very short time-steps. Thus, fully coupled models using process-based approaches can require prohibitively large computational resources to address hydrologic questions even at the scale of a river basin (Kollet and Maxwell 2008; Niu et al. 2014).

Additionally, there are relatively few models available that simulate GW and lake interactions as a function of climate and land use. One modular finite-difference coupled SW/GW model was recently developed (Markstrom et al. 2008) and applied successfully to a lake-rich region, estimating water budget components for several lakes (Hunt et al. 2013). This data-intensive approach relied on relatively high horizontal and vertical resolution as well as detailed calibration of soil and aquifer characteristics to match lake and GW elevation observations. The need to include such detail (and collect the data to calibrate the model) creates obstacles when attempting to model larger regions and often limits case studies to relatively small research watersheds that have been extensively characterized in field studies.

Recognizing the need for a spatially explicit, yet computationally parsimonious, modeling framework, we have developed a regional-scale hydrologic simulation model, which couples SW, GW, and lake water budget (LWB) models in an integrated framework. This modeling framework: (1) captures the unique water budgets of numerous individual lakes, (2) does

so with limited input data, (3) is scalable to large spatial analyses, and (4) runs on readily available computer resources.

The overarching objective for the development of this modeling framework was to support ecological modeling that was dependent on hydrologic fluxes (e.g., lake carbon processing; Zwart et al. 2018). The simplicity of our approach was intended to facilitate application of the model to relatively large spatial scales and we demonstrated this capability by applying it to a lake-rich region (6,400 km^2; 3,692 lakes) on the border of northern Wisconsin and Michigan in the United States (U.S.). With our modeling framework, we addressed two primary research questions: (1) Can a simplified LWB modeling approach be devised that compares well to observed datasets and simulations from more complex models? (2) What are the relative roles of SW and GW fluxes in determining the varying hydrologic behavior of lakes within a large spatial region?

METHODS

Modeling Overview

We evaluated our modeling framework by comparing simulated hydrologic outputs to observed datasets as well as simulations from a more complex integrated SW/GW model. The novel modeling framework we developed for simulating LWBs couples readily available SW and GW models yielding hydrologic fluxes that were used to drive a simple LWB model, newly developed for this application. The general flow of information within the integrated SW/GW modeling framework is shown in Figure 1. We give a brief overview of the integrated framework here, and subsequent sections describe each sub-model in more detail.

Inputs included publically available geographical, geological, and daily meteorological data, and the model simulates major daily water fluxes into and out of each lake within the region at a daily time-step. We ran the macroscale Variable Infiltration Capacity (VIC) hydrologic model (Liang et al. 1994; Liang et al. 1996) once across the entire region, producing daily aggregated values of precipitation, run-off, baseflow, ice cover, snow storage and melt, open water evaporation, and GW recharge. We one-way coupled VIC to the analytic element method (AEM) GFLOW GW model (Haitjema 1995), using simulated GW recharge values from VIC as forcings for GFLOW. GFLOW then generated estimates of daily GW discharge for each lake. We then one-way coupled VIC at daily time-step to our spatially explicit LWB model for other hydrologic fluxes into and out of
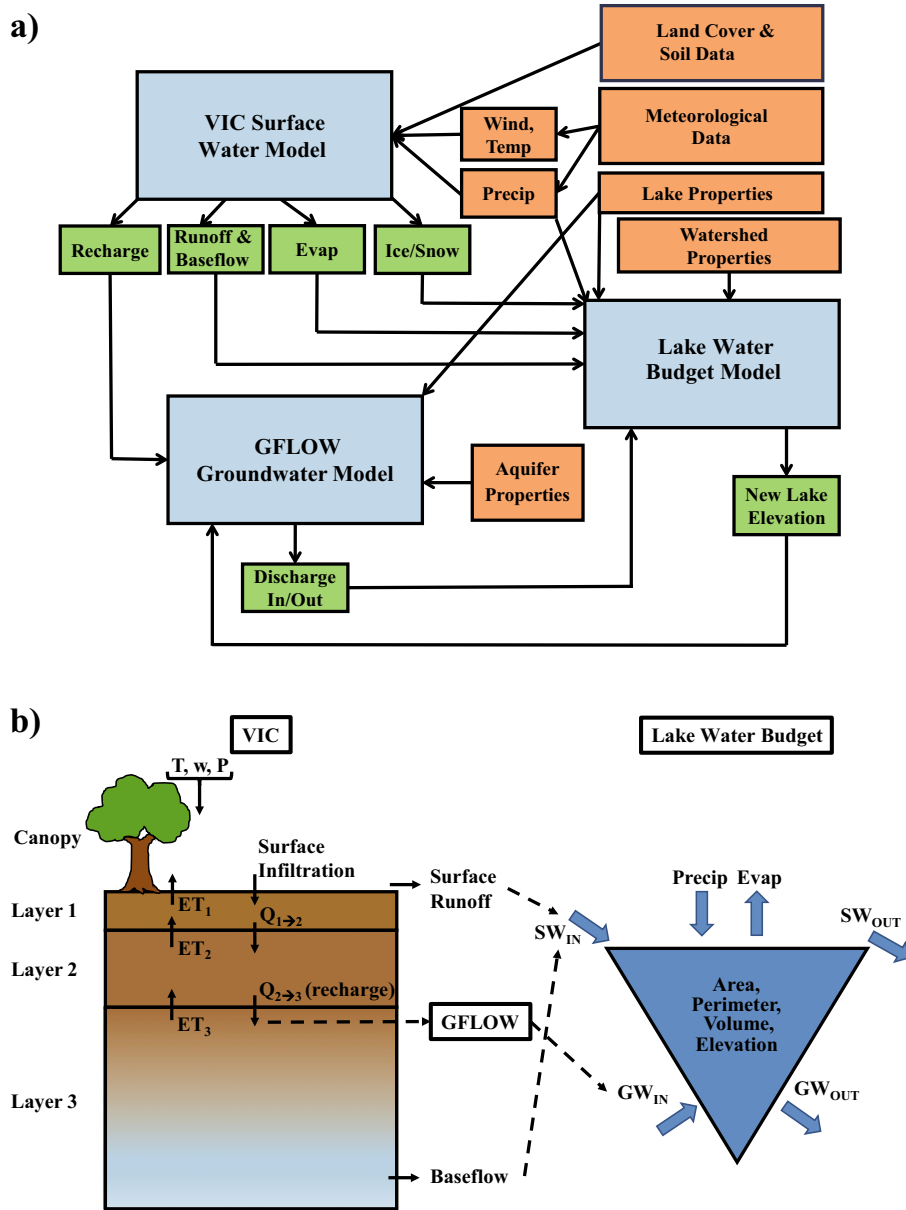
FIGURE 1. (a) Schematic diagram of integrated surface water (SW), groundwater (GW), and lake water budget (LWB) model with the various input datasets and properties used for each. Orange boxes represent forcing and model setup data inputs, blue boxes represent the individual models, and the green boxes represent fluxes and information moving between the models. (b) Visualization of the model connections and transfer of information between the models. VIC, variable infiltration capacity.

the lake. Using the combined fluxes from VIC and GFLOW, we simulated the resulting changes in lake storage and lake surface elevation with our LWB model. We two-way coupled the GW and lake models at a monthly time-step through the updating of lake surface elevation boundary conditions in GFLOW.

Study Site

To establish proof of concept, we applied our integrated lake model to the Northern Highlands Lake District (NHLD) located in northern Wisconsin and the Upper Peninsula of Michigan (Figure 2a, 2b), and simulated daily LWBs for every lake across water years (WYs) 1980–2015 (October 1, 1979–September 30, 2015). We chose this region due to extensive validation data that were available and because it is an ecologically important site, characterized by a very high proportion of lake areal coverage on the landscape (13%; Peterson et al. 2003). The site is broadly representative of many north temperate and boreal landscapes around the globe. The NHLD has been the focus of many hydrologic (e.g., Hunt et al. 1998;
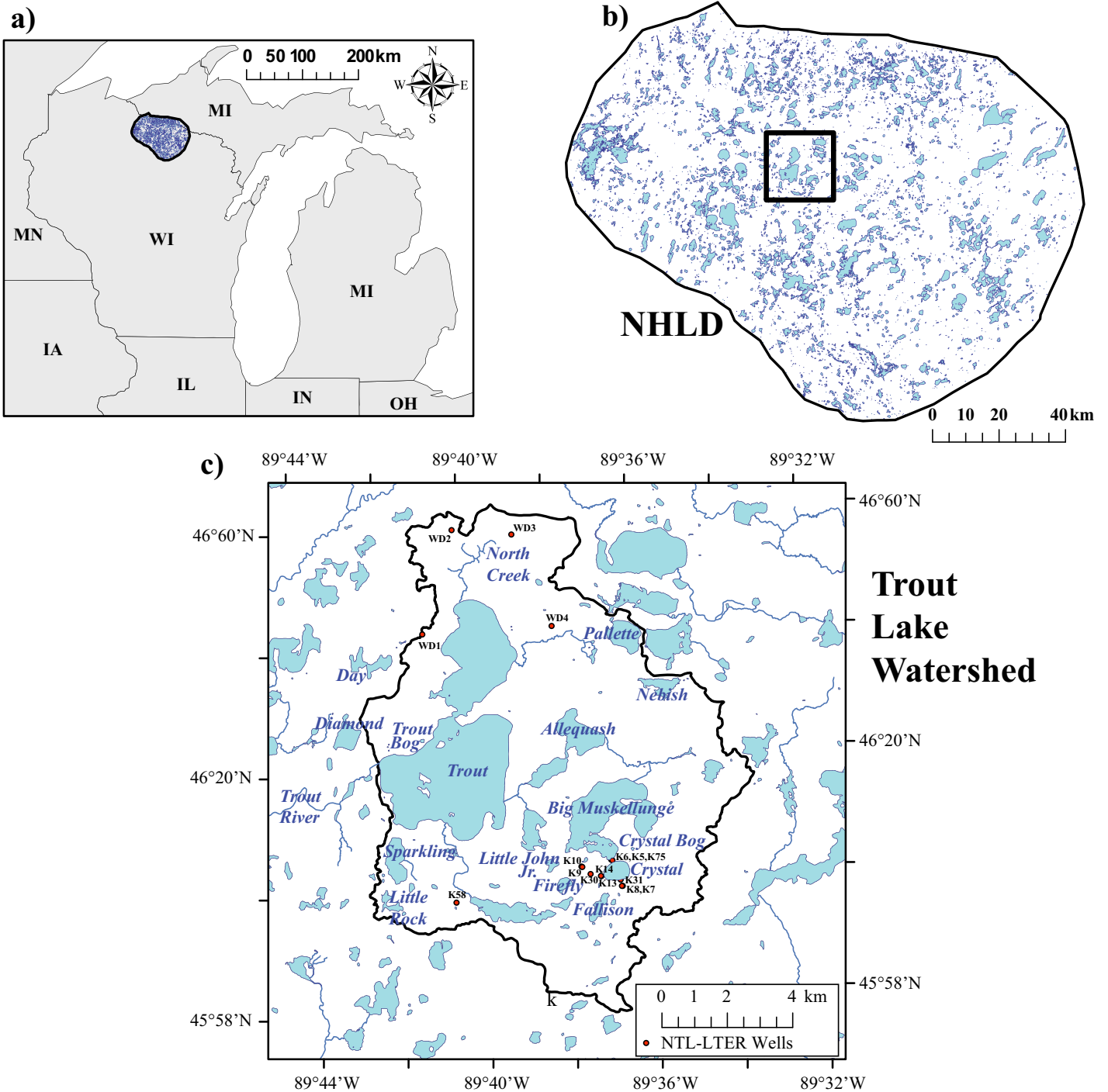
FIGURE 2. (a) The Northern Highlands Lake District (NHLD) location along the northern WI and MI border is shown in blue with black outline. This region is a lake-rich area (6,400 km² containing nearly 4,000 lakes). (b) Extent of the NHLD with the 3,692 lakes simulated (SIM) in this study with the Trout Lake Watershed outlined in black. (c) North Temperate Lakes Long Term Ecological Research (NTL-LTER) subset of lakes and wells used in analysis for this study within the Trout Lake Watershed. Black line denotes the hydrologic unit code 12 boundary. Orange dots display location of NTL-LTER observation wells used in our analysis. MI, Michigan; MN, Minnesota; WI, Wisconsin; IA, Iowa; IL, Illinois; IN, Indiana; OH, Ohio.

Pint 2002; Hunt et al. 2006; Muffels 2008; Hunt et al. 2013) and limnological studies (e.g., Striegl et al. 2000; Houser et al. 2003; Jones et al. 2009; Hanson et al. 2014), with the bulk of the focus on water bodies in the centrally located Trout Lake Watershed that serve as focal systems for the North Temperate

Lakes Long Term Ecological Research site (NTL-LTER; Magnuson et al. 2006; https://lter.limnology.wisc.edu/).

The core NTL-LTER hydrologic data focus on the Trout Lake Watershed, including lake surface elevation for five lakes and two bog lakes as well as nearly 40 GW monitoring wells (Figure 2c). This made for an ideal site to apply our model and test its ability to capture the hydrologic characteristics of this diverse set of lakes, including *drainage lakes* with water budgets dominated by SW fluxes (Allequash Lake and Trout Lake); *seepage lakes* with water budgets dominated by precipitation, evaporation, and GW fluxes (Big Muskellunge Lake, Crystal Lake, and Sparkling Lake); and smaller *bog lakes* (Crystal Bog and Trout Bog) that are often isolated from the local GW system (Wetzel 2001, chapter 25), and whose net water inputs are therefore dominated by precipitation and evaporation alone.

SW Modeling

We used version 4.1.2.g of the VIC macroscale hydrologic model as our SW model. We obtained the soil and vegetation parameter datasets from previously published work (Livneh et al. 2013) which provided VIC input data for the conterminous U.S. based on the land data assimilation system project datasets (Mitchell et al. 1999). VIC solved the land surface energy and water balance for each 1/16th degree grid cell (roughly 7×5 km) at daily time-steps. Each VIC grid cell consisted of (1) a vegetation layer which represented a mosaic of land cover classes, (2) a top soil layer (typically 10 cm in depth) that controlled surface infiltration and runoff, (3) a middle soil layer which represented the unsaturated vadose zone (typically 30 cm in depth), and (4) a bottom soil layer (typically 0.5–2.5 m in depth) which represented variations in the water table height that control GW inputs to streams as baseflow (Figure 1b). Fluxes of water at the surface due to infiltration and between the three soil layers were calculated at a daily time-step.

Similarly, VIC simulated both surface runoff and baseflow, expressed as a depth for each grid cell (Figure 1b). Total volumetric streamflow discharge was estimated by combining these two values together over a given contributing watershed area (WA). For calibration (parameterization detailed in Appendix E; Table E.2), surface runoff and baseflow were added together and routed using VIC's simple routing model (Lohmann et al. 1996) for a large watershed within the NHLD. We simulated lake ice cover, snow storage, and snowmelt using the lake model available in VIC (Bowling and Lettenmaier 2010; further detailed in Appendix A).

We estimated GW recharge from VIC as the net amount of water moving between the middle (vadose zone) and the bottom (GW) soil layers (Q_{23}; Figure 1b) due to drainage and diffusion arising from soil moisture gradients. Evapotranspiration from the third soil layer (ET_3) was subtracted from Q_{23} to estimate net GW recharge, which we used to force GFLOW. That is:

$$\text{net GW recharge} = (Q_{23} - ET_3). \quad (1)$$

Writing the mass balance of the third soil layer we obtain:

$$\Delta SM_3 = Q_{23} - ET_3 - B_3, \quad (2)$$

where ΔSM_3 is the change in soil moisture in layer 3, and B_3 is the baseflow (GW input to streams) from layer 3. Which implies:

$$\text{net GW recharge} = (Q_{23} - ET_3) = (\Delta SM_3 + B_3). \quad (3)$$

Thus in the long-term mean, net GW recharge should approximately equal B_3, because the storage term becomes negligible.

Additional details on *Surface Water Modeling* methods are detailed in Appendix A, including: (1) meteorological driving data input and the associated energy and water fluxes calculated, (2) the VIC soil parameter calibration and streamflow comparison, and (3) the modeling of a representative lake within the NHLD to capture seasonal lake ice and snow storage and melt dynamics using the VIC lake model.

GW Modeling

We implemented the AEM steady-state GW modeling approach using version 2.2.2 of GFLOW for our GW model. We modeled the NHLD aquifer as a homogeneous 50 m thick single layer of glacial sand and gravel on top of impermeable bedrock (Attig 1985) with a high degree of connectivity between the GW storage and the SW features throughout the domain. We used GFLOW to solve the two-dimensional steady-state GW equation (Haitjema 1995; equation 3.152) with the variable inputs being lake elevations and the daily average recharge forcing rate across a given month from VIC output. The outputs of interest in our integrated modeling framework were GW discharges into and out of each lake. We represented lakes as discretized polygons with each

lakeshore section being an individual *analytic element*. We set elevations of the analytic elements (lake surface elevations) based on monthly output from the LWB model as boundary conditions to GFLOW. By using available geospatial polygons and elevation data, we were able to quickly and simply construct our modeling domain. This straightforward approach can be readily scaled to large spatial extents in support of regional- or even global-scale analyses.

The AEM takes advantage of the linear nature of the GW equation; using the principle of linear superposition, the total steady-state GW flow solution can be solved by adding together the steady-state solutions for GW potential associated with each analytic element. The AEM solution was updated each month to balance tradeoffs between run time and the ability of the model to capture intraseasonal variations in GW fluxes to the lakes with reasonable fidelity. However, when first attempting to use the AEM steady-state solution for each monthly time-step, we encountered a fundamental problem. The steady-state solution from the AEM, with a daily average recharge forcing rate across a given month, caused the GW system to instantaneously jump from one steady-state solution to another. By doing so, the response time needed in reality for the GW system to move from one state to another was not accounted for. As a result, the steady-state solution added or removed water from the system far too quickly. To resolve this, we applied a transient approximation through the use of a recharge adjustment based on mass balance of stored water in the saturated layer and net recharge (details in Appendix B). In essence, this *quasi-transient* model constrained the steady-state GW mounding simulated by GFLOW so that it matched the theoretical GW storage volume that would occur after a month of recharge.

Practical limits on the size of GFLOW implementations, the need to scale up to regional or global domains, and the desire to facilitate computational efficiency using parallel computing, motivated us to split the GW model domain into discrete subdomains that were each solved on an individual processor. We based these subdomains on the Watershed Boundary Dataset 12-digit hydrologic units (HUC12s; https://water.usgs.gov/GIS/huc.html). GFLOW uses so-called *nearfield* and *farfield* boundary conditions, and we optimized the size of the subdomains for each HUC12 so that the GW simulations produced for lakes within single HUC12s closely matched simulations for the same lakes centrally located within larger modeling extents. By breaking the NHLD into subdomains, we allowed the AEM model to function much like a gridded model, such as VIC, in which the cells do not communicate. This computational structure is very easily parallelized. Additional details on this macroscale discretization process for the GW model are provided in Appendix B.

To simulate the individual subdomains, we applied uniform parameters for our GFLOW runs across the entire NHLD (Table E.2 in Appendix E). The local aquifer thickness used represents the homogeneous aquifer thickness for a given subdomain's nearfield and farfield lakes. To estimate the local average surface elevation, we used the average initial elevation of the nearfield lakes, with the base of the aquifer set 50 m below that estimated elevation (Attig 1985). This base elevation was necessary for GFLOW to solve for several parameters used in the calculation of discharge to or from each lake (Haitjema 1995; chapter 5). We set the total aquifer thickness to an arbitrarily large value (500 m) above the aquifer base elevation in order to ensure unconfined flow conditions in the GFLOW solutions. This was necessary for the chosen AEM method, which if hydraulic head were above the surface elevation would revert to an inappropriate confined-aquifer calculation. We tested two values of saturated hydraulic conductivity (1 and 10 m/day), based on a range of values reported for the region (Hunt et al. 1998; Pint 2002; Muffels 2008; Hunt et al. 2013). The larger value tended to provide GW fluxes that were an order of magnitude larger than typically reported for the NHLD (Pint 2002; Hunt et al. 2006; Muffels 2008; Hunt et al. 2013) and so the smaller value of 1 m/day was used. We used a lakebed resistance value that was previously implemented within AEM models of the Trout Lake Watershed (e.g., Hunt et al. 1998) for all lakes across the NHLD (Table E.2 in Appendix E). The other necessary input for GFLOW, in addition to the lake surface elevations, was net recharge (Equation 1). Because we ran GFLOW once for each month in order to provide estimates of daily average discharges, we averaged the net recharge rate from VIC output, as described above, and applied that rate uniformly across each corresponding HUC12 subdomain.

LWB Modeling

Integrated with the GW model, we simulated the LWB model for 88 subdomains across the NHLD region corresponding to the same HUC12-derived subdomains previously described in the GW modeling. We used ArcGIS version 10.1 (ESRI 2012) and the National Hydrology Dataset (NHD) to identify and select all lakes (Ftype 390) and reservoirs (Ftype 436; modeled as lakes) within the geographic extent of the NHLD boundary (https://lter.limnology.wisc.edu/dataset/north-temperate-lakes-lter-northern-highlands-lake-district-boundary). Since we were interested in

modeling complete water budgets for each lake and reservoir in the region, at the outset we chose to retain even the smallest lakes in our dataset. However, many small lakes were not accurately represented in the NHD (Soranno et al. 2015). To avoid problems, we manually inspected each lake and reservoir within the NHLD, comparing the NHD classification with Google Earth Imagery and the World Imagery Basemap in ArcGIS. Our final dataset included 3,692 lakes and reservoirs within the NHLD region (see Zwart et al. 2018 for more information on dataset inspection). We simulated each lake one time within its respective subdomain across the modeling time period and synthesized the results of all subdomains into a single regional dataset for subsequent analysis of the NHLD.

Our lake and reservoir dataset was projected in Arc-GIS using the U.S. Contiguous Albers Equal Area Conic projection in order to calculate the lake's initial area and perimeter. Since lake volume and bathymetry was unknown for most lakes in the NHLD (also regionally and globally), we estimated initial lake volumes by fitting a relationship between lake volume and lake area (LA) using data for 143 lakes within the NHLD:

$$V_{ini} = 10^{(-0.0589+1.1296 \times \log_{10}(A_{ini}))}, \quad (4)$$

where V_{ini} is the volume of the lake (m^3) and A_{ini} is the surface area of the lake (m^2). A right circular conical shape with a constant aspect ratio (a function of V_{ini} and A_{ini}) was used to estimate the bathymetry of each lake and the change in lake surface elevation as a function of simulated change in volume. We used data gathered from the Wisconsin Department of Natural Resources (https://dnr.wi.gov/lakes/lakepages/Results.aspx?location=NORTHERN), Hanson et al. (2007), and the NTL-LTER databases (https://lter.limnology.wisc.edu/dataset/north-temperate-lakes-lter-northern-highland-lake-district-bathymetry). Hanson et al. (2007) provided data for depth at sample site, and all other data were provided as mean depth for volume calculations. We provide details for obtaining our LA and volume dataset in Appendix F of the Supporting Information. In order to allow for daily runoff and baseflow values from VIC to be converted to daily volumetric SW and baseflow inflow rates (m^3/day), WAs (i.e., the total upstream catchment area feeding the lake) were calculated for each lake (see Appendix C for details). A small subset of the lakes (~1%) showed very large WA to LA (WA:LA) ratios, and these outliers were set to average WA to LA (WA:LA) ratios as described in Appendix C.

With all the hydrologic inputs, lake evaporation, and outflowing GW discharge determined by the SW and GW models, we calculated the daily mass balance of individual lakes using the equation:

$$\frac{\Delta V}{\Delta t} = P - E + SnwM$$
$$+ SW_{baseflow} + SW_{runoff} - SW_{out}$$
$$+ GW_{in} - GW_{out} \quad (5)$$

where $\frac{\Delta V}{\Delta t}$ is the change in lake volume per day (m^3/day), P is direct precipitation (rain and snow when ice cover is absent; m^3/day), E is open water evaporation from the lake surface (m^3/day), SnwM is the snowmelt on top of the ice that directly enters the lake (m^3/day), $SW_{baseflow}$ is inflowing baseflow from the lake's contributing WA (m^3/day), SW_{runoff} is inflowing surface runoff from the lake's contributing WA (m^3/day), SW_{out} is the outflowing SW (m^3/day), and GW is the GW flux (in and/or out; m^3/day).

All VIC output values used were by default expressed as a depth of liquid water over the grid cells; direct precipitation, evaporation, and snowmelt over ice were multiplied by the simulated LA for a given day, resulting in a volumetric flux. Inflowing SW fluxes were handled differently to apply the correct volumetric daily rate that flowed from the WA alone, rather than the LA. Lakes in our NHLD dataset were split into two classes (see Appendix C for details): (1) for lakes without stream channels ($n = 3,186$), daily total surface runoff from the VIC model was scaled to a lake's contributing WA, and (2) for lakes with stream channels ($n = 506$ within the NHLD), the sum of runoff and baseflow from the VIC model was multiplied by the contributing WA to estimate total streamflow entering the lake. Thus in seepage lakes, inflows from SW are intermittent and occur only when intense precipitation produces surface runoff, whereas lakes with stream inputs receive simulated baseflow between storms. We modeled lakes individually from one another without specified SW routing between lakes or storage within a lake's watershed. This simplifying approach still allowed for the inclusion of both $SW_{baseflow}$ and SW_{runoff} for the minority of lakes that drain the landscape, and efficient simulation of all lakes within our modeling framework. SW_{out} was modeled as a linear reservoir (Dingman 2015; equation 9-28) following:

$$SW_{out} = \begin{cases} \frac{(V-V_{ini})}{T^*}; & \text{if}(V-V_{ini}) > 0 \\ 0; & \text{if}(V-V_{ini}) \leq 0 \end{cases}, \quad (6)$$

where $(V - V_{ini})$ is the change in volume above the reference volume obtained from our reference lake surface for the beginning of the current daily time-step (V_{ini}; m^3) and T^* is a scaling parameter (day). In theory T^* should vary with LA, but because individual characteristics of lake outlets across the NHLD were mostly unknown and data were only available for three lakes in the region, the relationship between LA and T^* was not known with high certainty. We estimated

T^* using three natural drainage lakes within the NHLD for which we had volumetric and discharge time-series data, and the average of these three T^* estimates (16 days; minimum of 9, maximum 28) was applied to all lakes in the NHLD. Initial testing showed that the model was not very sensitive to uncertainty in T^*. Thus, given the limited data available, we chose this relatively simple approach.

Stabilizing the Simulation of Small Lakes, Perched Lakes, and Small Fluvial Drainage Lakes

When we first ran the LWB model fully integrated with GFLOW, it became clear that additional information was needed through several prescreening simulations in order to detect problematic parameter settings for specific lakes. In particular, the stability of small lakes (<1 ha; 10,000 m^2) was poor when GW fluxes were set at default values. The majority of these lakes dried out in the simulations, suggesting too high a connectivity between these lakes and the surrounding aquifer. To resolve this problem, we assumed small lakes had relatively small GW fluxes to or from the aquifer, which was incorporated in the model by setting a high lakebed resistance. Thus, very small lakes in the simulations were not strongly influenced by GW dynamics and are driven instead mostly by the balance between precipitation and evaporation, aligning with literature that documents that bogs were generally disconnected from GW fluxes (Wetzel 2001; chapter 25).

Briefly, small lakes (<1 ha; 10,000 m^2) as well as several larger perched lakes were assigned a high lakebed resistance value (essentially disconnecting them) in order to eliminate the unrealistic draining or filling initially seen due to simulated GW fluxes. In total, 1966 of the 3,692 total simulated lakes within the NHLD were disconnected, but these small lakes accounted for <1.3% of the NHLD by LA, which is in agreement with previous literature showing that this region is numerically dominated by small, perched lakes (Hanson et al. 2007). Similarly, small lakes that were located along river channels were initially unstable using the constant T^* that was estimated. The lakes used for the estimation had much larger storage than these very small, drainage lakes. To screen for these unstable lakes, we identified lakes whose volume doubled in a single day when a maximum daily SW inflow was imposed with the constant T^*. For these lakes ($n = 42$), we set daily SW outflow to SW inflow (SW$_{out}$ = SW$_{baseflow}$ + SW$_{runoff}$), mimicking the behavior of stream reaches. Details relating to these prescreening simulations are located in Appendix D.

Additional Details on Model Integration and Code Resources

Integrating a group of individual models using our methods described above created a framework for simulating detailed water budgets for individual lakes over large areas while maintaining a relatively parsimonious modeling framework. Appendix D in the Supporting Information provides the various model-simulated time periods for model calibration, initialization, and validation. Appendix E gives additional details on model integration and sequencing, and provides a flowchart for the order of operations of the integrated modeling. Appendix F describes availability of model source code including the LWB model and the various existing models (e.g., VIC, GFLOW) used in our modeling framework.

Overview of Model Validation Using Observed Data

We used a number of publicly available datasets from the NHLD to validate our modeling framework, including: (1) streamflow discharge, (2) lake ice duration, (3) GW elevations, (4) radon concentration measurements (proxy for inflowing GW), (5) lake surface elevations, and (6) estimated values of lake hydrologic residence time (HRT). Data for validation were primarily available in the Trout Lake Watershed (NTL-LTER; Figure 2c), and additional details regarding the various validation datasets are provided in Appendix G. The long-term, but spatially constrained, data within the Trout Lake Watershed were supplemented with a broader spatial survey of radon concentrations, which we used to validate our modeling of GW flux estimates for a broader subset of NHLD lakes. Radon measurements in lakes serve as an indicator of the relative importance of GW to a lake's water budget since radon concentrations in GW sources are several orders of magnitude higher than SW sources (Kluge et al. 2007; Dimova et al. 2013). Additionally, as GW flux in lakes can be spatially heterogeneous, estimating whole-lake GW flux using lake water column radon measurements has an advantage over more traditional (and labor-intensive) GW sample methods since they serve as an integrator of GW flux over the entire lake. We provide details for obtaining our radon dataset in Appendix F of the Supporting Information.

Published (PUB) lake HRT estimates (Hanson et al. 2014) were compared to simulated values from our study. HRT is a common variable of interest for many ecologic and hydrologic lake studies. We express HRT as:

$$\text{HRT} = \frac{\overline{V}}{\overline{P} + \overline{\text{SnwM}} + \overline{\text{SW}_{\text{baseflow}}} + \overline{\text{SW}_{\text{runoff}}} + \overline{\text{GW}_{\text{in},}}} \quad (7)$$

where V is lake volume (m^3), P is direct precipitation (rain and snow when ice cover is absent; m^3/day), SnwM is the snowmelt on top of the ice that directly enters the lake (m^3/day), SW$_{\text{baseflow}}$ is inflowing surface baseflow from the lake's contributing WA (m^3/day), SW$_{\text{runoff}}$ is inflowing surface runoff from the lake's contributing WA (m^3/day), and GW$_{\text{in}}$ is inflowing GW flux (m^3/day). The mean daily values for each hydrologic component are calculated for the entire simulation period in order to estimate a single representative value for each lake. For validation, we compared our simulated HRTs with previous HRTs for the five NTL-LTER lakes and two NTL-LTER bogs that were presented in Hanson et al. (2014), derived from observed bathymetry data (Hanson et al. 2014) and simulated hydrologic flux estimates (Hunt et al. 2013).

Overview of Model Validation Using Inter-Model Comparison

In addition to validation using observed data, we compared our simulations to a previous highly calibrated and detailed modeling effort in the Trout Lake Watershed (Hunt et al. 2013; Figure 2c). That study used GSFLOW (Markstrom et al. 2008) and an integrated Lake Simulation Package (Merritt and Konikow 2000) within MODFLOW-2005 (Harbaugh 2005) in order to model 30 lakes of interest within the Trout Lake Watershed. Calibrated and fully coupled results from the study included inflowing GW fluxes, net lake hydrologic budgets, model performance in comparison to observed data mentioned above (simulated lake surface and GW elevations), and mean lake surface elevations.

We validated our simulated GW fluxes to previously PUB estimates of GW inflow and outflow determined using stable-isotope analysis and steady-state mass balance techniques for 11 lakes in the Trout Lake Watershed (Ackerman 1992; Pint 2002; Hunt et al. 2006; Muffels 2008; Hunt et al. 2013). The samples were collected in 1991 and were representative of GW fluxes for the years prior to 1992. Additionally, we compared GW influx estimates produced by our relatively simple GW model to GW influx estimates from the calibrated and fully coupled model used by Hunt et al. (2013) over their calibration period from WYs 2000–2007. We also calculated average annual values of simulated net precipitation ($P + \text{SnwM} - E$), net SW (SW$_{\text{baseflow}}$ + SW$_{\text{runoff}}$ − SW$_{\text{out}}$), and net GW (GW$_{\text{in}}$ −

GW$_{\text{out}}$) for the five NTL-LTER lakes from WY 1980–2015 from our LWB model and compared to Hunt et al. (2013) estimates over the same time period (bog lakes were not included in the Hunt et al. 2013 study). Furthermore, we compared our simulated lake evaporation for Sparkling Lake to previous observations (Lenters et al. 2005) and simulations (Hunt et al. 2013).

Metrics for Model Performance

We used several metrics of model performance when comparing our simulated results to observation datasets as well as previously PUB modeling results. For comparison to time-series data, we used the Nash–Sutcliffe efficiency coefficient (NSE) and mean absolute error (MAE) to estimate a nondimensional (NSE) and dimensional (MAE) goodness of fit, respectively. Additionally, we used a correlation coefficient (r) to quantify how well our simulations captured time-series dynamics in observations. For streamflow, we computed a ratio of the means (simulated/observed) for baseflow-dominated periods (June–September) as a means for validating net GW recharge estimates from VIC. For across lake comparisons using long-term averages, we used MAE, r, or a combination of the two metrics. We provide details relating to the definitions of NSE and MAE in Appendix H.

Metrics for Summarizing Regional Lake Hydrologic Characteristics

An additional metric of interest for this study was the fraction of hydrologic export as evaporation (FHEE), expressed as:

$$\text{FHEE} = \frac{\overline{E}}{\overline{E} + \overline{\text{GW}_{\text{out}}} + \overline{\text{SW}_{\text{out},}}} \quad (8)$$

where we calculated the mean values for each of the exporting hydrologic components for the entire simulation period to estimate a single representative value. FHEE is a useful metric for lake ecological studies because it summarizes important LWB characteristics (high FHEE seepage lakes vs. low FHEE drainage lakes) and dominant water pathways, which have been shown to be influential in lake carbon cycling dynamics (Zwart et al. 2017; Jones et al. 2018). For regional analysis, we calculated linear regressions between HRT, FHEE, and WA:LA for all lakes within the NHLD. To evaluate the results from our modeling framework at regional scales, we compared HRT estimates with global estimates (Messager et al. 2016) as well as a relationship with WA:LA from an extensive observation survey performed within Wisconsin (Lillie and Mason 1983).

RESULTS

Model Validation Based on Observed Data and Inter-Model Comparison

Despite minimal calibration and uniform parameters applied to each of our individual SW, GW, and LWB models, our integrated modeling framework performed well when compared to observations and previous highly calibrated modeling results. Varying hydrologic behavior between lake types was successfully captured as well as estimates of elevations and fluxes. Specifically, elevations of GW and lake surface levels and fluxes of GW and areal processes (net precipitation) were in reasonable agreement with observations and simulated results of Hunt et al. (2013).

Streamflow for a small creek draining into Trout Lake reproduced baseflow periods better than peak flows (Figure 3). Lake ice duration for the seven NTL-LTER lakes captured interannual dynamics ($r > 0.78$), but was biased high overall (Figure 4 and Table 1). Ice duration for the smaller bog lakes best matched the representative lake used for simulating the lake ice, whereas Trout Lake had a MAE value of 23.7 days and Trout Bog had a MAE value of 9.4 days. GW observation wells located closer to lakes (NTL-LTER labeled "K" wells) matched simulations better than wells located further from lake boundaries (NTL-LTER labeled "WD" wells; Figure 5, Table 2, Figure I.1 and Table I.1 in Appendix I of the Supporting Information).
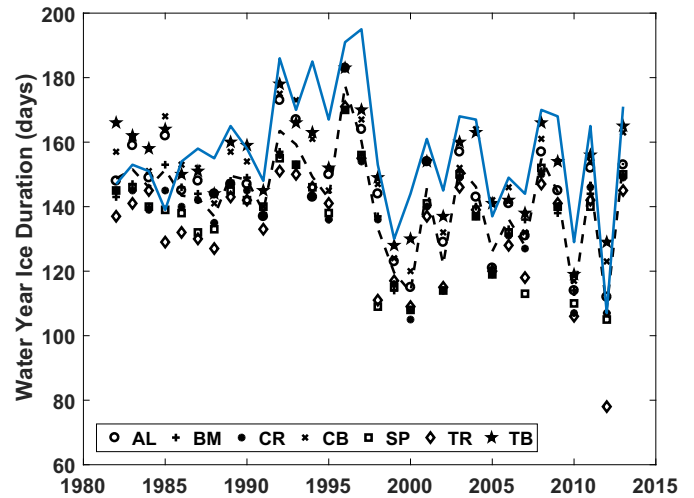
FIGURE 4. Lake ice duration from WYs 1982–2013. Dashed black line represents the mean value for all seven of the NTL-LTER lakes and bogs. OBS durations for individual lakes are represented with various symbols (see Table 1 for lake name abbreviations). Simulated values for a single lake (blue) using the VIC lake model with parameterization in Table E.2 of the Supporting Information Appendix E.

Excluding Big Muskellunge, our average outflowing GW discharges over the entire simulation period were positively correlated across lakes with observations of average daily GW fluxes derived from stable-isotope analysis (Figure 6; $r = 0.64$). Outflowing GW discharge estimates improved slightly when looking at the years prior to 1992 (WYs 1988–1991; $r = 0.71$). Hunt et al. (2013) did not provide outflowing GW discharge estimates. Simulated inflowing GW discharges (excluding Big Muskellunge) were not significantly correlated across lakes with isotope data at 95% confidence ($r = 0.45$, $p = 0.19$), but were a better match with observations than model results produced by Hunt et al. (2013) ($r = -0.09$, $p = 0.81$). The very small sample size of the isotope derived data was an important driver of significance in these statistics. Additionally, variation in GW fluxes to individual lakes, as measured by radon levels, was positively correlated to modeled inflowing GW discharge (Figure 7; $r = 0.76$), demonstrating that the model was capable of distinguishing the GW/SW characteristics for a larger group of lakes outside of the Trout Lake Watershed.

Estimates of net precipitation, net SW, and net GW for the five NTL-LTER lakes successfully captured net hydrologic flux direction (i.e., influx or efflux) from Hunt et al. (2013; Figure 8). Net precipitation from our model was equal for all of the NTL-LTER lakes, as the model did not account for any variations in rates between lakes. Previous Sparkling Lake evaporation estimates over a 10-year analysis
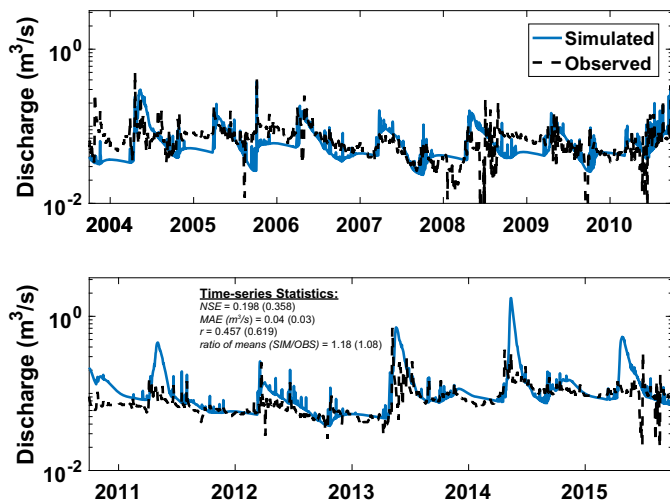

FIGURE 3. VIC SIM (blue) North Creek discharge inflowing to Trout Lake compared to observations (black) over water years (WYs) 2004–2015. Statistics for the full time-series are provided, with baseflow periods (June–September) presented in parentheses. NSE, Nash–Sutcliffe efficiency; MAE, mean absolute error; OBS, observed.

TABLE 1. NTL-LTER ice duration and lake surface elevation results.

Lake	Allequash Lake (AL)	Big Muskellunge Lake (BM)	Crystal Bog (CB)	Crystal Lake (CR)	Sparkling Lake (SP)	Trout Bog (TB)	Trout Lake (TR)
Ice duration							
NSE	0.436	0.319	0.543	0.313	0.285	0.628	0.294
MAE (days)	13.8	18.4	10.9	19.9	21.2	9.4	23.7
r	0.788	0.783	0.785	0.815	0.814	0.811	0.885
n	32	32	32	32	32	32	32
Lake surfaces							
NSE	−0.071	−2.672	−0.035	0.576	−3.432	0.003	0.153
MAE (m)	0.26	0.38	0.20	0.25	0.29	1.35	0.12
r	0.050	0.466	0.437	0.915	0.393	0.685	0.549
n	438	427	431	437	406	445	344
Hunt et al. (2013) lake surfaces							
NSE	−0.079	0.933	—	0.953	0.946	—	0.430
n (estimated)	120	105	—	100	115	—	100
Lake surfaces (modified)							
NSE	−0.079	0.025	−0.038	0.645	0.556	0.206	0.155
MAE (m)	0.25	0.67	0.20	0.18	0.21	0.12	0.12
r	0.052	0.629	0.440	0.884	0.835	0.682	0.548
n	438	427	431	437	406	445	344

Note: Lake ice duration time-series for SIM results over WYs 1982–2013 and lake surface elevation time-series for SIM results over WYs 1980–2015. Hunt et al. (2013) results are presented for lake surface elevations (excluding bog lakes). The lake surface elevation results are also presented after modifications detailed in the discussion (see Effects of Improved Information on Model Simulations) were implemented for the Trout Lake Watershed subdomain.
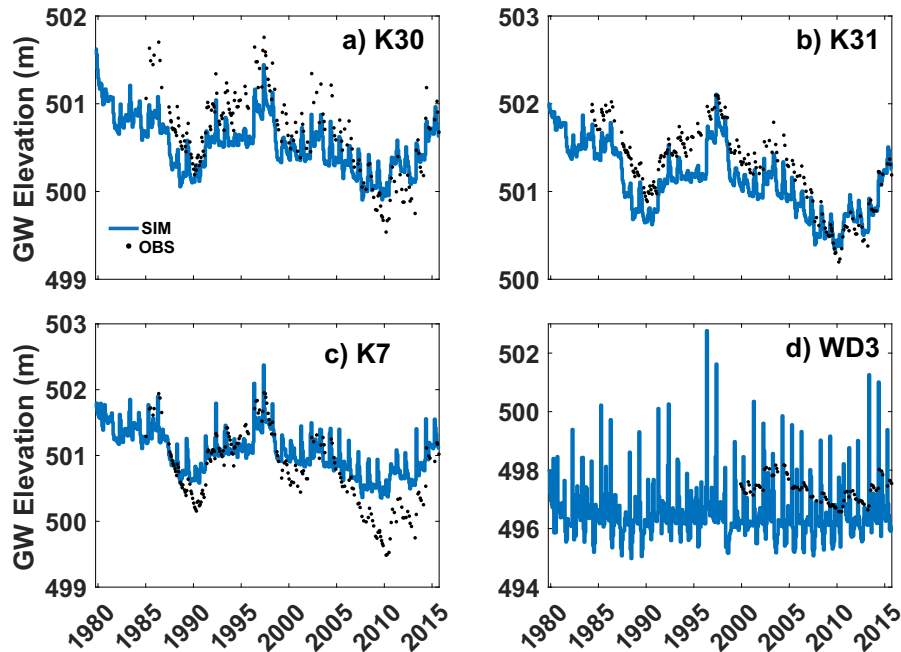

FIGURE 5. Time-series plots of simulated (blue) values representing one-month steady-state GW elevations compared with OBS (black dots) GW elevations (meters above NAVD88) for 4 (a–d) of the 16 observation wells included within the Trout Watershed Basin from WYs 1980–2015. See Appendix I in the Supporting Information for the additional well results. NADV, North American Vertical Datum.

(Lenters et al. 2005; June 21–September 27, WYs 1989–1998) had a mean and standard deviation of 3.4 and 0.2 mm/day, respectively. Our results overpredicted lake evaporation for Sparkling Lake with a simulated mean and standard deviation of 5.0 and 1.0 mm/day, respectively, but were more consistent with results presented by Hunt et al. (2013). Additionally, our net precipitation estimates were nearly

TABLE 2. NTL-LTER GW elevation results.

Well ID	NSE	Hunt et al. NSE	MAE (m)	r	Difference of means (SIM-OBS) (m)	n	σ_{SIM} (m)	σ_{OBS} (m)	Range$_{SIM}$ (m)	Range$_{OBS}$ (m)
K30	0.078	0.524	0.29	0.874	−0.21	204	0.28	0.47	1.54	2.22
K31	0.499	—	0.27	0.919	−0.24	215	0.36	0.45	1.78	1.90
K7	−0.171	−5.475	0.33	0.800	0.22	203	0.33	0.57	2.02	2.47
WD3	−0.131	−0.161	1.30	−0.097	−0.73	90	1.24	0.41	6.08	1.60

Note: Hunt et al. (2013) results are also provided for a comparison between several wells. Hunt et al. (2013) statistics are based on 35–45 values for each well and did not provide results for several wells used in this study (e.g., K31). See Appendix I in the Supporting Information for the additional well results.
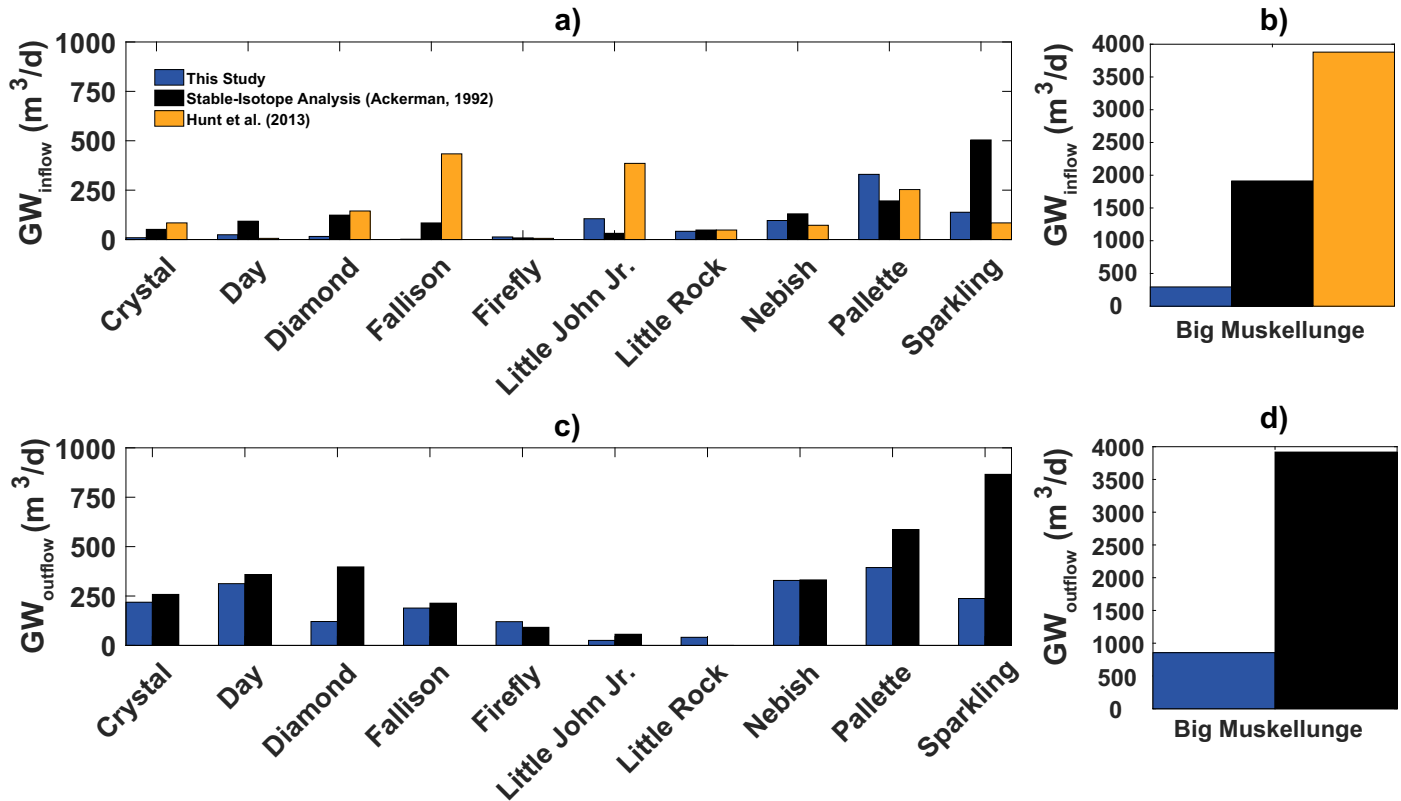

FIGURE 6. Our model-simulated daily average inflowing GW over WYs 1980–2015 (blue) compared with stable-isotope analysis estimates representative prior to 1992 (black) as well as estimates from Hunt et al. (2013; yellow) for (a) 10 of the lakes in the Trout Lake Watershed, and (b) Big Muskellunge only. Our model-simulated daily average outflowing GW over WYs 1980–2015 (blue) compared with stable-isotope analysis estimates representative prior to 1992 (black) for (c) 10 of the lakes in the Trout Lake Watershed, and (d) for Big Muskellunge only.

identical to Hunt et al. (2013) for Trout Lake. Net SW estimates from Hunt et al. (2013) were greater than our model estimates for the drainage lakes (Allequash Lake and Trout Lake), especially for Allequash Lake. Our model estimates of net GW more closely matched estimates from Hunt et al. (2013) for seepage lakes, while net GW from both of the drainage lakes were lower than estimates from Hunt et al. (2013).

Our integrated modeling framework also successfully captured seasonal dynamics of lake surface elevations for the seven NTL-LTER lakes and bogs

(Figure 9 and Table 1) as well as mean lake surface elevations for the five NTL-LTER lakes and 22 additional lakes in the Trout Lake WA (Table 3). The simulations of Crystal Lake (Figure 9a) performed the best with NSE, MAE (m), and r values of 0.576, 0.25, and 0.915, respectively, and successfully captured the decadal cycles seen in observations. The model also performed well for drainage lakes (Figure 9d, 9e and Table 1) and bog lakes (Figure 9f and 9g and Table 1), although there was bias between the initial elevation and the observed elevation for Trout Bog due to the choice of initial conditions. Mean lake
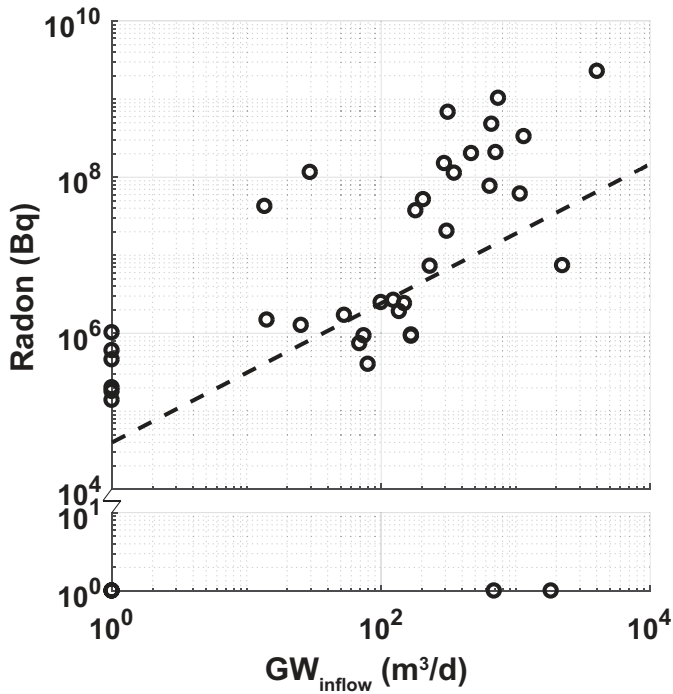
12

FIGURE 7. OBS radon measurements compared to average SIM daily inflowing GW discharges over WYs 2014–2015 for the 40 lakes surveyed across the NHLD during open water periods of 2015 and 2016. Near zero values for radon measurements and SIM inflowing GW discharges were set to a value of 1.0 in order to display low-end performance of the model (radon only, $n = 2$; SIM inflowing GW only, $n = 6$; both, $n = 2$). The dashed black line represents log~log linear regression best-fit line. Bq, Becquerel.

surface elevation for the 5 NTL-LTER as well as 22 non-NTL-LTER lakes (17 of which have no inflowing or outflowing drainage features from within the NHD dataset) captured the average conditions compared to PUB observations, even performing substantially better than the calibrated coupled modeled results from Hunt et al. (2013) for some lakes (Table 3).

Lastly, a majority of simulated HRT estimates for the five LTER lakes and two LTER bogs did not agree with previously PUB values (Table 4). However, they did not appear to contain a preferential direction of bias and are likely due to random errors in lake volume (see further analysis and discussion below in Effects of Improved Information on Model Simulations).

Evaluation of Simulated Lake Hydrologic Characteristics over the NHLD

A majority of lakes in the NHLD had a simulated mean and median annual HRT of less than two years (1.68 and 1.63 years, respectively; Figure 10a and Table 5). Volume-weighted mean HRT for the region was 2.38 years (dashed vertical line in Figure 10a). These values were broadly consistent with previous studies estimating HRT across a global dataset of lakes (Messager et al. 2016), as well as within Wisconsin, where a survey of Wisconsin lakes estimates that seepage and drainage lakes have a mean HRT of 2.15
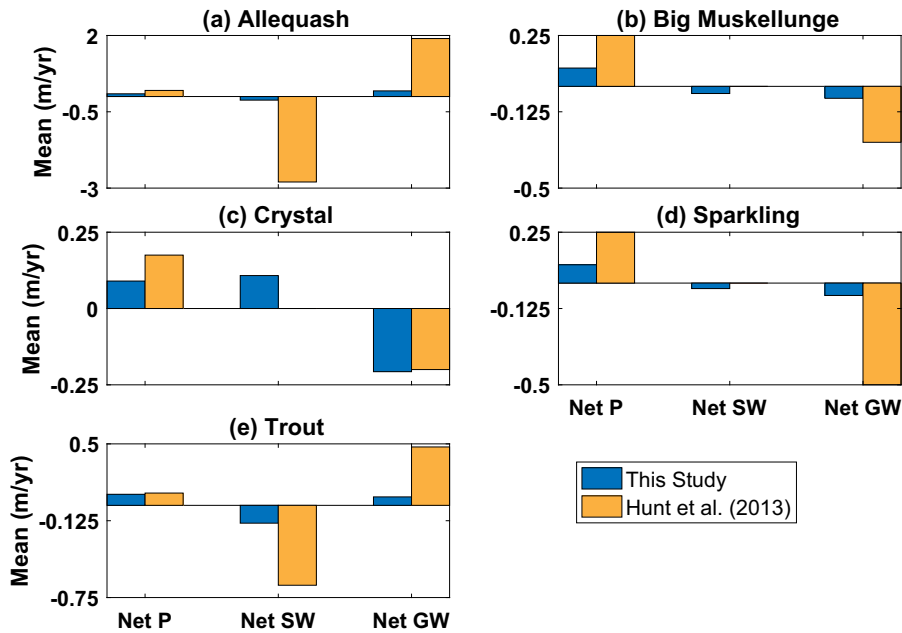

FIGURE 8. Our model-simulated (blue) average annual rates normalized by lake area (LA) for net precipitation (P), net SW, and net GW for the five NTL-LTER lakes (a–e) compared with Hunt et al. (2013) model estimates (yellow).
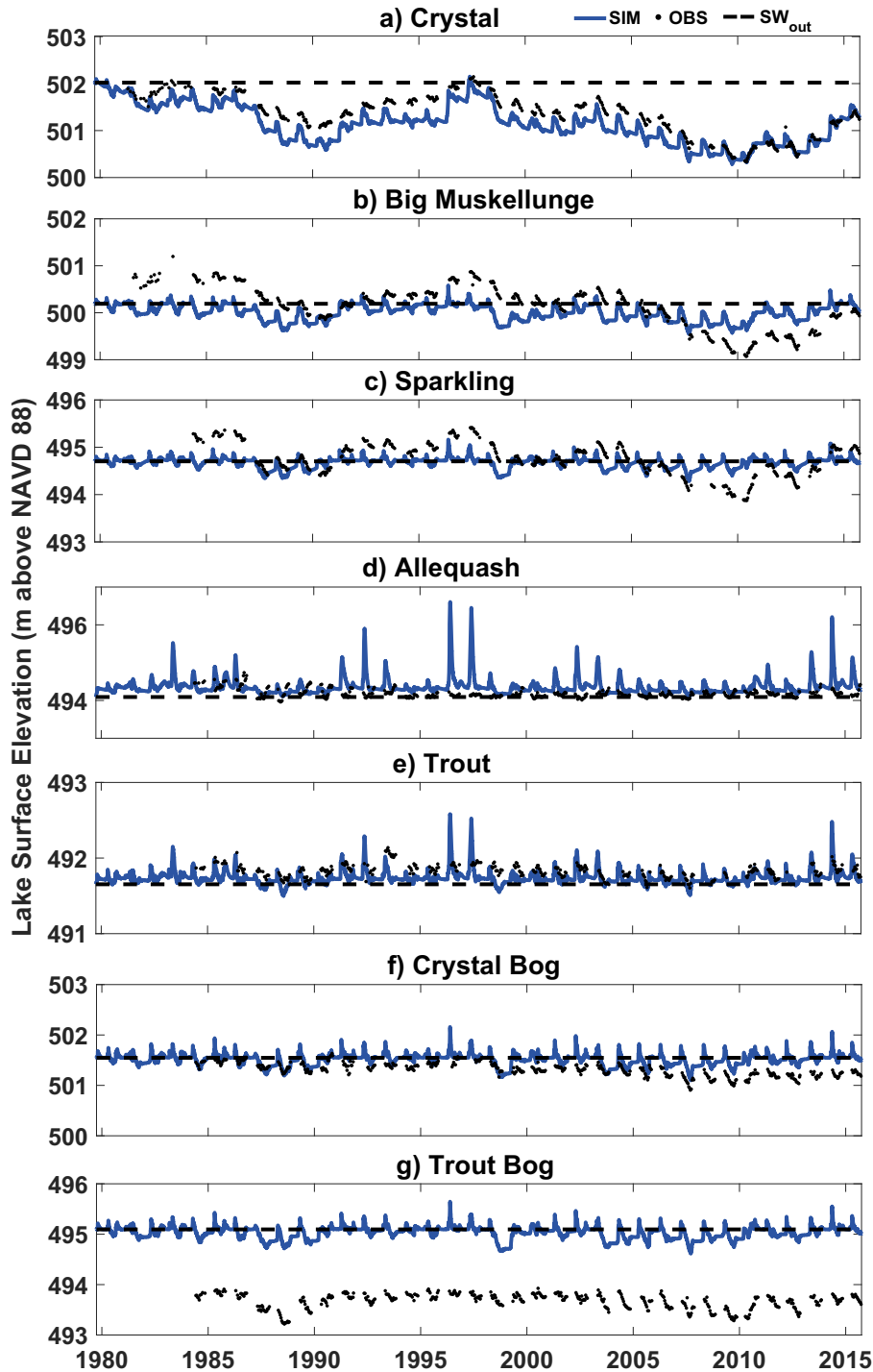
FIGURE 9. Complete integrated SW, GW, and LWB model daily SIM (blue) lake surface elevations compared with OBS (black dots) for (a–c) seepage lakes, (d and e) drainage, and (f and g) bogs over WYs 1980–2015. The black dashed horizontal line represents the elevation at which surface outflow is SIM to begin and where the lake elevations initialize.

and 1.42 years, respectively (Lillie and Mason 1983). Our simulated lake HRT was negatively correlated to WA:LA (Figure 10b; $r = -0.29$) and was positively correlated with the FHEE (Equation 8; Figure 10c; $r = 0.81$). FHEE was also negatively correlated to WA: LA (Figure 10d; $r = -0.35$). These results were consistent with the negative relationship between HRT and WA:LA observed by Lillie and Mason (1983).

TABLE 3. Mean lake surface elevation result statistics for the 5 NTL-LTER lakes as well as 22 additional lakes within the Trout Lake watershed area (WA).

	All data		Two outliers removed	
	This study	Hunt et al. (2013)	This study	Hunt et al. (2013)
MAE (m)	0.37	0.51	0.30	0.15
Max AE (m)	1.38	6.38	0.94	0.67

Note: Values are averaged across the entire simulation period (WYs 1980–2015) and presented for all 27 lakes considered as well as removing the two most extreme outliers.

DISCUSSION

Lakes are important features on the landscape as they provide societal benefits through recreation, drinking water, food, and nutrient cycling, among many others. Understanding how lakes and the services they provide will change in response to changing climate and surrounding watershed characteristics requires well-integrated hydrologic models suitable for application over a wide range of spatial scales. Unfortunately, most integrated hydrologic models to date are limited to smaller watersheds because they are computationally intensive. These limitations in current modeling frameworks are an obstacle to understanding how lakes in aggregate will change across a region. To this end, we have developed a spatially explicit model capable of estimating daily hydrologic fluxes for thousands of lakes in a region. Despite uniform parameters applied across the entire model domain (Appendix E; Table E.2), our model performed well when compared to observations and more sophisticated model simulations of hydrologic fluxes and elevations. The two research questions we aimed to address relating to performance of our simple modeling framework and the hydrologic variation across an extensive lake population are detailed throughout our discussion. Below we discuss the model performance, the simulated regional lake hydrologic characteristics of the NHLD, and explore where there is room for improvement in our current modeling framework.

Model Performance

LWB Performance. The model developed for this study explicitly simulated important hydrologic processes for lake studies including GW discharges, SW baseflow, SW runoff, lake surface evaporation, as well as ice cover and snowmelt in order to compute the entire water budget for each lake of interest. From the simulated change in volume, the change in surface elevation was then simulated using an estimated bathymetry for each lake. Using uniform parameters, daily lake elevations for the hydrologically diverse set of lakes seen in the NTL-LTER were well captured. Although model performance metrics did not match exactly with the more sophisticated modeling

TABLE 4. A comparison of SIM and published (PUB) lake characteristic values for the five LTER lakes and two LTER bogs for original and modified SIM results: SIM LA, SIM lake volume, PUB mean depth (Hanson et al. 2014), derived PUB volumes as the product of SIM area and PUB mean depth, volume correction ratio (SIM/PUB), SIM hydrologic residence time (HRT), PUB HRT, volume adjusted SIM HRT using the presented volume correction ratio, and SIM HRT using derived PUB volumes as well as modifying parameterization for several lakes (see Effects of Improved Information on Model Simulations for modified parameters).

Lake	SIM area (km^2)	SIM volume (10^3 m^3)	PUB mean depth (m)	PUB derived volume (10^3 m^3)	Volume ratio (SIM/PUB)	SIM HRT (year)	PUB HRT (year)	Volume adjusted SIM HRT (year)	Modified parameterization SIM HRT (year)
Allequash[1]	1.64	9.18E+03	3.2	5.25E+03	1.75	0.79	—	0.45	0.47
Allequash Upper[1]	1.12	5.96E+03	3.2	3.58E+03	1.66	0.56	0.73	0.34	0.35
Big Muskellunge	3.76	2.33E+04	7.5	2.82E+04	0.83	5.74	5.1	6.94	7.99
Crystal Bog	0.006	1.50E+01	1.7	1.02E+01	1.47	1.79	1.42	1.22	1.12
Crystal	0.375	1.73E+03	10.4	3.90E+03	0.44	4.02	11	9.06	10.47
Sparkling	0.637	3.14E+03	10.9	6.94E+03	0.45	3.13	8.88	6.91	10.79
Trout Bog	0.01	2.91E+01	5.6	5.60E+01	0.52	2.10	4.67	4.03	4.06
Trout	15.8	1.19E+05	14.6	2.31E+05	0.51	2.59	5.28	5.04	4.94

[1]We simulated the total lake basin area of Allequash Lake. Hanson et al. (2014) presented values representative of the upstream basin only. To allow for direct comparison of HRT we simulated: (1) the total area of Allequash Lake with our default volume estimation and parameterization (SIM), (2) the total area of Allequash Lake with volumes based on Hanson et al. (2014) reported mean depth for the upper basin, as well as (3) the upstream basin of Allequash Lake with our default volume estimation and parameterization (SIM), and (4) the upstream basin of Allequash Lake with volumes based on Hanson et al. (2014) reported mean depth for the upper basin. The upstream basin was SIM with a LA (1.12 km^2) and perimeter (5.9 km, about 63% of our perimeter length estimated for the total basin) adjusted to match values reported by Hanson et al. (2014).
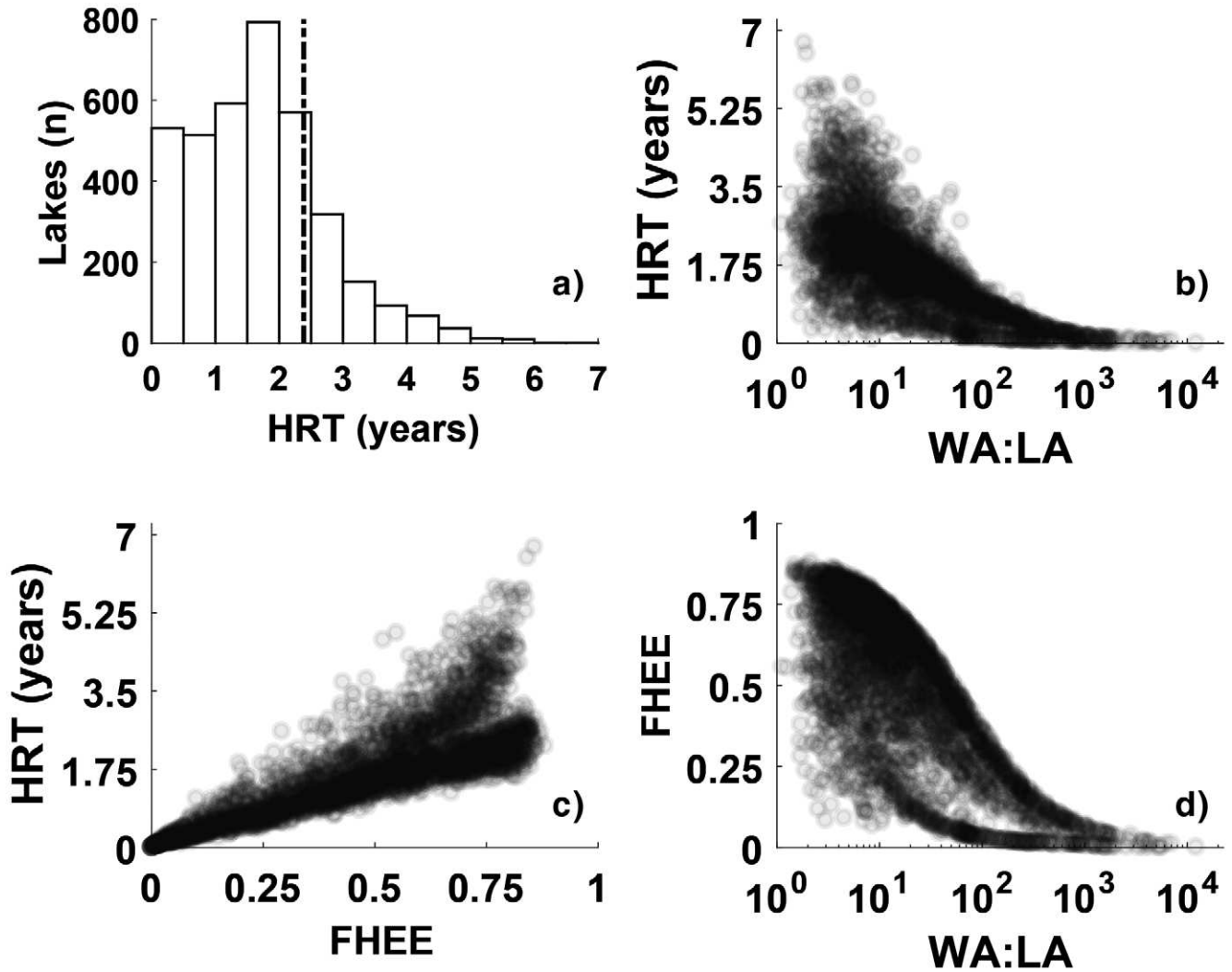
FIGURE 10. Regional lake HRT relationship with several lake and landscape hydrologic metrics for the 3,692 lakes within the NHLD. (a) HRT histogram with volume-weighted mean shown by the vertical dashed black line. (b) HRT vs. WA to LA (WA:LA). (c) HRT vs. fraction of hydrologic export as evaporation (FHEE). (d) FHEE vs. WA:LA. Each gray circle represents a lake long-term mean hydrologic characteristic over WYs 1980–2015.

TABLE 5. Regional lake morphometric and hydrologic characteristics for the NHLD summarized using minimum (Min), maximum (Max), and quartiles for each variable: geospatial initial LA (A_{ini}); WA; estimated mean depth from initial area (A_{ini}) and volume (V_{ini}); SIM HRT; fraction of export as evaporation (E), SW outflows, and GW outflows; fraction of inputs as direct precipitation (P) and snowmelt (SnwM), SW inflows, and GW inflows.

Variable	Min	0.25	0.50	0.75	Max
A_{ini} (10^3 m^2)	0.06	2.06	10.30	73.16	6.75e+04
WA (10^3 m^2)	0.68	46.23	242.27	1.22e+03	2.21e+06
Mean depth (m)	1.47	2.35	2.89	3.73	9.04
HRT (years)	<0.01	0.89	1.63	2.26	6.71
Fraction export as E	<0.01	0.28	0.52	0.69	0.88
Fraction export as SW	0	0.13	0.33	0.65	>0.99
Fraction export as GW	0	<0.01	0.03	0.17	0.93
Fraction input as P and SnwM	<0.01	0.32	0.59	0.78	0.98
Fraction input as SW	<0.01	0.08	0.18	0.41	0.99
Fraction input as GW	0	0	0.01	0.11	0.90

approach for all lakes (Table 1), our results were within reasonable agreement, especially considering the model was not calibrated to any observed lake or GW elevations. Additionally, drought cycles seen within the 36-year time period were present and lake elevation response to these drivers was more prominent in seepage lakes than drainage lakes, which was supported by observations (Figure 9). These results show that our model was capable of capturing a range of lake types and hydrologic characteristics using very limited information about the lakes themselves.

Although our model performed well for several of the lakes with observation data, it was also clear that estimates of LWBs and related lake characteristics were not entirely correct for every lake. Several kinds of systematic model bias were noted in our simulations of lake surface elevation, including: (1) imperfect agreement of our simulated decadal variability in seepage lake elevations, (2) low bias in Big Muskellunge Lake and Sparkling Lake, especially for the highest elevations during decadal upswings associated with wet conditions, and (3) a systematic high bias in our Trout Bog simulations.

Imperfect agreement between simulations of decadal variability in lake surface elevation for Big Muskellunge, Sparkling Lake, and Crystal Lake and observations was likely related to multiple factors, including errors in lake volume, lake bathymetry (specifically area to volume relationships; Equation 4), WA:LA, and the assumed presence or absence of streams. For example, geospatial data showed that Big Muskellunge had an outflowing stream, Sparkling Lake had an inflowing stream, and Crystal Lake had neither. However, previous modeling studies with site knowledge from field studies have assumed that there was no streamflow into and out of any of the NTL-LTER seepage lakes (e.g., Hunt et al. 1998; Hunt et al. 2013). Due to the modeling assumption relating to the SW_{out} criterion, we under-simulated filling rates during decadal upswings in the simulated lake surface elevation time-series for both Big Muskellunge Lake and Sparking Lake (Figure 9b, 9c). These upswings were clearly evident in observations, but the simulated lake surface elevations for these two lakes were limited by the designated V_{ini} values controlling SW_{out}. Similarly, the discrepancies between our simulated SW fluxes for all NTL-LTER lakes and Hunt et al. (2013) simulations were likely related to the assumptions of both V_{ini} and T^* model parameters. The apparent systematic errors in our Trout Bog simulations of lake surface elevation were likely due to errors in the reference datum for the observed dataset. It should also be noted that our case study region has relatively small topographic gradients, which increases the difficulty in delineating flowlines and watersheds. These kinds of errors might be less important in other regions.

SW Inflow Performance. Our simulated streamflow for the small creek flowing into Trout Lake showed good overall agreement with observations. Although our simulation performed poorly in reproducing peak streamflow for some years (Figure 3), this was expected given that the creek drainage area was relatively small and observed precipitation stations that were used to produce the gridded meteorological driving dataset for the macroscale VIC model were outside the watershed's contributing basin area. Specifically, the model captures peak flow events well from 2004 to 2010, and relatively poorly from 2011 to 2015, which again suggests errors in the driving data rather than the model itself. It is important to note that such errors are common at small spatial scales unless local-scale precipitation data can be obtained, and thus an exacting reproduction of the historical time-series was not to be expected.

The Sparkling LWB discrepancies were likely explained by the imperfect simulation of small stream inputs as seen in the streamflow analysis. Having an inflow in the geospatial data resulted in both VIC runoff and baseflow as hydrologic inputs to the lake under our model's current setup. VIC forcing data errors or calibration could also be at fault, especially when applied to these small-scale watersheds.

GW Performance. Traditional transient GW models are computationally expensive, especially when implemented at the high resolution needed to capture the behavior of small lakes. Because of this, we developed a quasi-transient solution to modeling lakes across a large region using an AEM steady-state GW model at monthly time-steps. GW elevation extracted from our simulations agreed well with observations for most GW wells located near lake boundaries, which was expected and desired in order to simulate GW discharges with high fidelity. Our estimated daily inflowing and outflowing GW discharges also agreed with observed GW discharges used in previous literature (Pint 2002; Hunt et al. 2006; Muffels 2008) as well as highly detailed modeling results of Hunt et al. (2013). We also observed good correlation between radon concentrations and simulated inflowing GW discharges for a majority of the 40 lakes we sampled across the NHLD, which demonstrated that the model can accurately characterize the balance between SW and GW inputs over a wide range of lakes. From this, we infer that our quasi-transient approximation using a steady-state AEM code is acceptable for our specific goal of estimating LWBs within the NHLD.

As noted earlier, challenges in simulating the transient response for smaller lakes and bogs were

encountered, and improving these aspects of the model will be the subject of future work. The use of initial uniform parameters for lake bed resistance (Appendix E; Table E.2) throughout the domain caused some small lakes to drain completely within a few days in the simulations. These modeling artifacts were likely exacerbated by the monthly time-step in the GW modeling used to estimate daily GW fluxes, which is possibly too long for small lakes, resulting in unstable simulations of lake volume storage. To avoid these problems in our current work, small lakes were hydrologically disconnected from the GW system by setting the effective lake bed resistance to a high value (Table E.2 in Appendix E). This adjustment was not believed to be a significant issue because these small lakes often sit high in the watershed and are at the center of old peat bogs and thus water exchange with the regional GW was likely very limited (Wetzel 2001; chapter 25). The radon data that we had for small lakes (<1 ha; 10,000 m^2) from the NHLD also indicated little GW inflow, providing additional support for this modeling decision. Another potential source of error in this context was the approach used to mimic the transient GW response based on the assumption of a characteristic distance between all water bodies for GW mounding. By making this assumption, correction for mass in the GW mounding may be overestimated in some places and underestimated in others, and more explicit representation of this parameter across the GW modeling subdomains could be investigated in the future.

Lake Ice Duration Performance. Considering that highly calibrated models (e.g., Magee et al. 2016) still have errors on the order of days to weeks, our simulations of lake ice duration performed quite well in comparison with the range of lake observations, despite the use of a single representative lake in the VIC simulations. Some overall high bias in the simulated lake ice duration results (Figure 4 and Table 1) was expected because the mean depth of the NHLD was skewed low due to the high count of small lakes and bogs in the region (Table 5). When we simulated the VIC lake model for depths more closely spanning the range of mean depths from NTL-LTER lakes, we saw improvements in mean error of lake ice duration. Although simulation of lake ice duration and snow accumulation and melt was relatively insensitive to LA, it was sensitive to both depth and latitude (location within the NHLD). Simulations exploring the sensitivity of lake ice duration to these two parameters over the range of NTL-LTER mean depths and the NHLD latitudes showed variation on the order of 4–7 days from the duration we estimated with our current parameters derived from a single representative lake.

Effects of Improved Information on Model Simulations

Using uniform parameters and publically available data, our model simulated lake surface elevation and hydrologic fluxes well when compared to NTL-LTER data for five lakes and two bogs. Here, we demonstrate potential model improvement by adding in some lake-specific information, which was not available for the entire set of lakes in the region. The modified results demonstrate that our model simulations can be improved with more detailed lake information without altering the model framework. Specifically, we:

1. Eliminated Big Muskellunge, Crystal Lake, and Sparkling Lakes' SW inflow and outflows by forcing them to be zero.
2. Set Trout Bog's starting surface elevation to the mean observed elevation.
3. Set the seven NTL-LTER lakes and bog volumes to volumes calculated with mean depths reported by Hanson et al. (2014) (Table 4).
4. As Hanson et al. (2014) only presented results for Allequash Lake's upstream basin, we simulated the total area of Allequash Lake as well as only the upper basin for HRT comparison using LA and perimeter values presented in that work.

Modified lake surface elevation simulations show the model improvements (Figure 11 and Table 1). The time-series of Big Muskellunge and Sparkling Lake surface elevation improved considerably without the presence of SW fluxes and decadal trends and seasonal drawdowns for Big Muskellunge, Sparkling Lake, and Crystal Lake all improved throughout the time-series (Figure 11a–11c and Table 1). Notably, even with the decadal trends more apparent, Big Muskellunge did have a slight overprediction of lake surface elevation throughout a majority of its time-series. We hypothesize that this was largely due to the underprediction of estimated outflowing GW when compared to observed values (Figure 7d) and highly detailed model estimates (Figure 8b). Improvements for Trout Bog were also readily seen through the agreement in seasonal drawdowns over many years, better aligning with observations after the bias was removed (Figure 11g).

Additionally, HRT is an important variable for lake studies, and errors for initial volumes for the lakes were determined to adversely affect the predictions of lake HRT for specific lakes. Volumes calculated with our regressed LA to volume relationship (Equation 4) often resulted in drastically different values compared with volumes calculated with LA and mean depth from field observations (Table 4). These errors
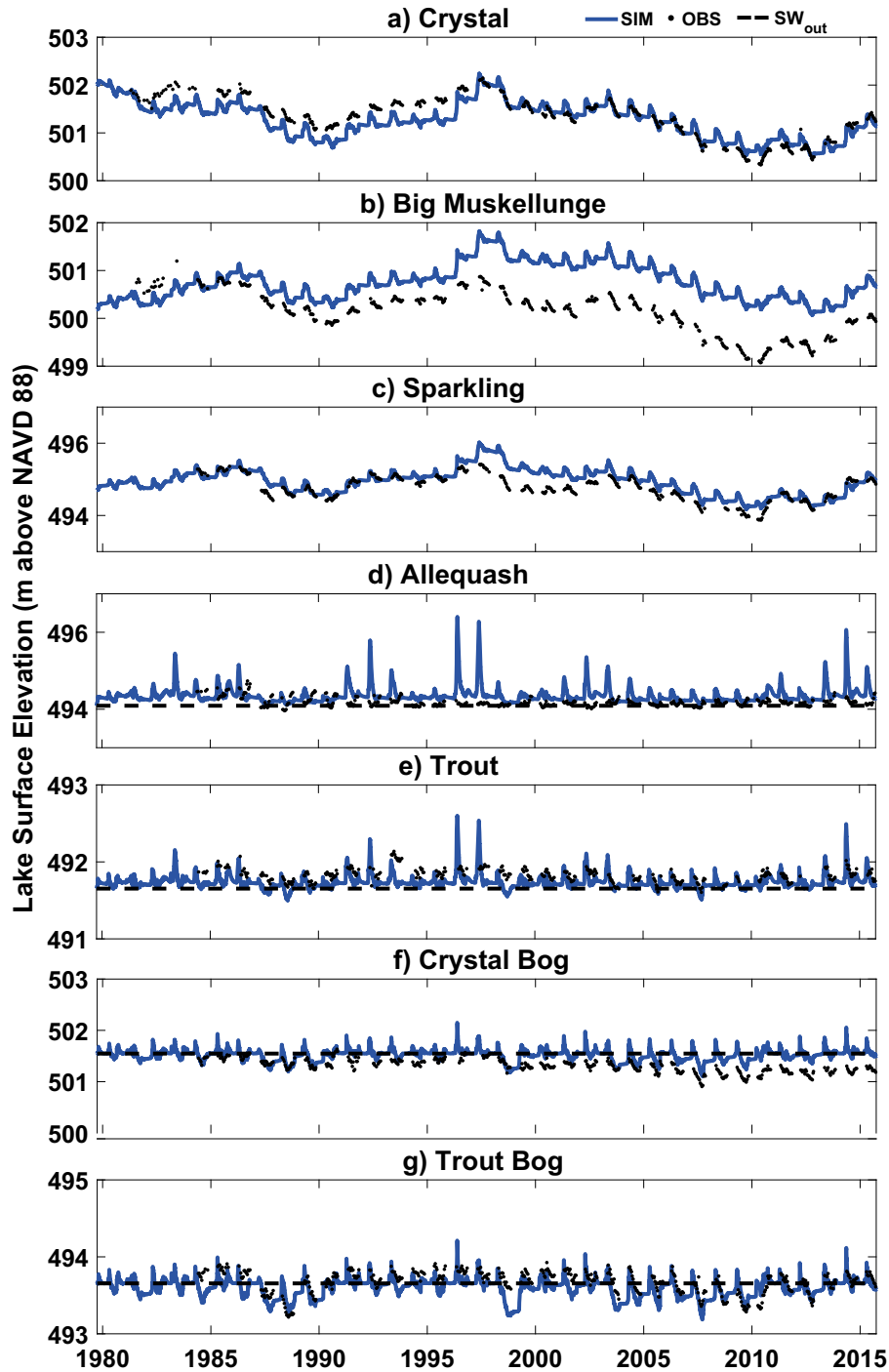
FIGURE 11. Modified complete integrated SW, GW, and LWB model daily SIM (blue) lake surface elevations compared
with OBS (black dots) for (a–c) seepage lakes, (d and e) drainage, and (f and g) bogs over WYs 1980–2015. The black dashed horizontal
line represents the elevation at which surface outflow is SIM to begin SW inflow and outflow was eliminated for the seepage lakes (a–c).

were primarily artifacts of the uncertain relationship
between area and volume used in our study, and
were essentially random. Unfortunately, more
detailed volume data are typically unavailable (Oliver
et al. 2016), but these issues clearly highlight the
need for improved estimation of lake volume that can
accurately measure lake volume over large spatial

scales in a cost-effective manner (e.g., via remote
sensing).

Improvements in HRT estimates varied across the
NTL-LTER lakes when we added detailed information
from field studies by substituting lake volume esti-
mates reported by Hanson et al. (2014) for V_{ini}
(Table 4). In the case of Allequash Lake, we note that

Hanson et al. (2014) only presented information representative of the upstream lake basin (Allequash Lake's lower basin was also included in our modeling by default). Initially, our simulated values of HRT for the total Allequash Lake basin aligned with the PUB value corresponding to the upstream basin. When we simulated only the upstream basin and corrected for volume, our model underestimated HRT. These discrepancies were likely because of errors in watershed delineation leading to a high bias in inflowing SW inputs, and with the high SW inputs, our initial HRT agreement was due to overestimating volumes. When we eliminated SW fluxes for the NTL-LTER seepage lakes, the results for Crystal Lake and Sparkling Lake improved markedly. Trout Lake and Trout Bog also improved significantly with their respective volume corrections.

These experiments further showed that overall estimates of SW and GW fluxes were relatively accurate. Errors in lake surface elevations were primarily due to errors in the local-scale SW characteristics, especially lake WA. These errors in SW characteristics often had their primary source in publically available geospatial datasets (e.g., presence and absence of streams), and products that were derived from these resources. Errors in lake specific HRT estimates were primarily due to lake volume uncertainty, which will remain unavoidable until technology for regional-scale lake bathymetry measurement is developed.

Regional Lake Hydrologic Characteristics

Summary for the NHLD. With our model, we were able to estimate daily water budgets for every lake within the NHLD, allowing us to examine both local and regional connections between lakes and their surrounding landscape that have not been previously examined at this level of detail for a large number of lakes. For example, a majority of lakes in the NHLD were classified as seepage lakes (hydrologic flux dominated by precipitation and evaporation), since the median FHEE value was 0.52 (Table 5). Seepage lakes are less connected to their surrounding landscape hydrologically than drainage lakes, and the degree of connectedness to the landscape can mediate regional drivers of lake water quality (Zhang et al. 2012; Read et al. 2015). Estimating the connectedness of lakes to their landscape for a region can help researchers and managers know which lakes are most vulnerable to changes in landscape characteristics such as conversion to agriculture. HRT has also been shown to have a strong influence on lake biogeochemical processing (Jones et al. 2018). For example, lake HRT determined the response of lake carbon cycling dynamics to extreme precipitation events (Zwart et al. 2017), and HRT often sets terrestrial carbon loading rates to lakes at longer time scales (e.g., Dillon and Molot 1997; Brett et al. 2012). Using our model, we can begin to more accurately estimate carbon loading from the landscape to lakes and estimate, in aggregate, lake contributions to regional carbon cycling within the NHLD (Zwart et al. 2018) as well as other regions of interest.

Model Application to Other Regions. It is difficult to determine *a priori* if the regional characteristics and performance of a modeled system can be generalized to other systems under varying hydrologic conditions. The NHLD region incorporates a wide range of lake and landscape characteristics and because of this we hypothesize that results from regions with varying hydrologic conditions will be comparable to those we have presented here. While our modeling approach performs well for the NHLD case study explored in this paper, and should work well for many hydrologically similar regions, future efforts should also focus on other regions with different SW and GW features, including for example, large lakes, mountainous landscapes, high latitude areas, and semiarid environments in order to test the portability of this model to other lake-rich regions.

Given that the SW and GW models and methods have been tested extensively in various conditions (Bakker et al. 1999; Maurer et al. 2002; Strack 2003; Hunt 2006; Livneh et al. 2013; Livneh et al. 2015), the uncertainties regarding application to other regions arguably pertain most clearly to the performance of the relatively simple coupling between SW/GW models and GW/LWB models used here. For example, use of the moisture flux between soil Layer 2 and 3 in the VIC model as a surrogate for net GW recharge (Equation 1 and Figure 1b) may not be appropriate in semiarid regions for which the water table is far below the surface. Future work to explore the applicability of these concepts to other environments may suggest alternate approaches.

The VIC SW model is dependent on relatively high-quality meteorological driving data. Where *in situ* meteorological observations are unavailable, simulations from regional-scale climate model simulations, or large-scale reanalysis simulations, could be substituted. For remote areas where streamflow observations are unavailable, calibration of the SW model could likely be omitted without major impacts on model performance (Figure 3 and Figure A.1 in Appendix A). The current modeling framework was designed to seamlessly incorporate climate and land use change, and can be straightforwardly applied at local and regional scales within any region of the U.S., or even globally, where necessary model setup and forcing data are available.

CONCLUSIONS

The ability to estimate the hydrologic characteristics of individual lakes is crucial in addressing hydrologic and ecologic questions relating to, for example, water resource management, transport and processing of organic constituents, and resulting ecosystem impacts. Our spatially explicit, process-based model is both parsimonious and efficient, requiring relatively little initial input data, which enabled simulations of thousands of LWBs at daily time scales. One key reason for this efficient modeling was the use of the alternative AEM GW modeling method, which allowed for quick and simple model construction. We validated our model using several observed datasets and previous sophisticated numerical studies that existed for a subset of lakes in the region of interest. Our analysis of nearly 4,000 lakes in northern Wisconsin and Michigan showed that our model was capable of estimating important lake hydrologic characteristics that can help to facilitate research in both hydrological as well as ecological fields using inputs that are widely available. A direct application of our integrated modeling framework to the ecological field has been detailed in Zwart et al. (2018), which used the hydrologic fluxes simulated in this study to investigate lake carbon processing for the same set of inland lakes. In this study, we also showed that our model can easily take advantage of new data sources to improve model performance. Future work is needed to test whether the performance of this approach is robust in different hydrologic settings, but the initial results from this study are very encouraging.

SUPPORTING INFORMATION

Additional supporting information may be found online under the Supporting Information tab for this article: Appendix A: Details of Surface Water Modeling; Appendix B: Details of Groundwater Modeling; Appendix C: Details of Watershed Delineations; Appendix D: Details of Modeling Simulations; Appendix E: Details of Modeling Framework Sequencing and Parameterization; Appendix F: Model Source Code and Data Availability; Appendix G: Details of the Model Validation Observation Datasets; Appendix H: Details of Metrics for Model Performance; and Appendix I: Additional NTL-LTER Groundwater Elevation Results.

DATA AVAILABILITY

The development code is available at the GitHub repository https://github.com/zhanson/NHLD_LWB_Model, and the code used to generate data in this manuscript was from v1.0.0, https://doi.org/10.5281/zenodo.1298746.

LITERATURE CITED

Ackerman, J.A. 1992. "Extending the Isotope Based (δ18O) Mass Budget Technique for Lakes and Comparison with Solute Based Lake Budgets." MS thesis, University of Wisconsin–Madison.

Attig, J.W. 1985. "Pleistocene Geology of Vilas County, Wisconsin." Wisconsin Geological and Natural History Survey Information Circular 50. https://wgnhs.uwex.edu/pubs/download_ic50/.

Bakker, M., E.I. Anderson, T.N. Olsthoorn, and O.D. Strack. 1999. "Regional Groundwater Modeling of the Yucca Mountain Site Using Analytic Elements." *Journal of Hydrology* 226 (3–4): 167–78. https://doi.org/10.1016/S0022-1694(99)00149-3.

Bixio, A.C., G. Gambolati, C. Paniconi, M. Putti, V.M. Shestopalov, V.N. Bublias, A.S. Bohuslavsky, N.B. Kastelteseva, and Y.F. Rudenko. 2002. "Modeling Groundwater–Surface Water Interactions Including Effects of Morphogenetic Depressions in the Chernobyl Exclusion Zone." *Environmental Geology* 42 (2–3): 162–77. https://doi.org/10.1007/s00254-001-0486-7.

Bowling, L.C., and D.P. Lettenmaier. 2010. "Modeling the Effects of Lakes and Wetlands on the Water Balance of Arctic Environments." *Journal of Hydrometeorology* 11 (2): 276–95. https://doi.org/10.1175/2009JHM1084.1.

Brett, M.T., G.B. Arhonditsis, S. Chandra, and M.J. Kainz. 2012. "Mass Flux Calculations Show Strong Allochthonous Support of Freshwater Zooplankton Production Is Unlikely." *PLoS ONE* 7 (6): e39508. https://doi.org/10.1371/journal.pone.0039508.

Crawford, N.H., and R.K. Linsley. 1966. "Digital Simulation in Hydrology Stanford Watershed Model IV." Technical Report No. 39. Palo Alto, CA: Department of Civil Engineering, Stanford University.

Dillon, P.J., and L.A. Molot. 1997. "Dissolved Organic and Inorganic Carbon Mass Balances in Central Ontario Lakes." *Biogeochemistry* 36 (1): 29–42. https://doi.org/10.1023/A:1005731828660.

Dimova, N.T., W.C. Burnett, J.P. Chanton, and J.E. Corbett. 2013. "Application of Radon-222 to Investigate Groundwater Discharge Into Small Shallow Lakes." *Journal of Hydrology* 486: 112–22. https://doi.org/10.1016/j.jhydrol.2013.01.043.

Dingman, S.L. 2015. *Physical Hydrology* (Second Edition). Long Grove, IL: Waveland Press.

ESRI (Environmental Systems Resource Institute). 2012. *ArcMap 10.1*. Redlands, CA: ESRI.

Feldman, A.D., P.B. Ely, and D.M. Goldman. 1981. "The New HEC-1 Flood Hydrograph Package." *U.S. Army Corps of Engineers Report No. TP-82*. http://www.hec.usace.army.mil/publications/TechnicalPapers/TP-82.pdf.

Haitjema, H.M. 1995. *Analytic Element Modeling of Groundwater Flow*. San Diego, CA: Academic Press.

Hanson, P.C., I. Buffam, J.A. Rusak, E.H. Stanley, and C. Watras. 2014. "Quantifying Lake Allochthonous Organic Carbon Budgets Using a Simple Equilibrium Model." *Limnology and Oceanography* 59 (1): 167–81. https://doi.org/10.4319/lo.2014.59.1.0167.

Hanson, P.C., S.R. Carpenter, J.A. Cardille, M.T. Coe, and L.A. Winslow. 2007. "Small Lakes Dominate a Random Sample of Regional Lake Characteristics." *Freshwater Biology* 52 (5): 814–22. https://doi.org/10.1111/j.1365-2427.2007.01730.x.

Harbaugh, A.W. 2005. "MODFLOW-2005, The U.S. Geological Survey Modular Ground-Water Model — The Ground-Water Flow Process." *U.S. Geological Survey Techniques and Methods 6-A16*. https://pubs.usgs.gov/tm/2005/tm6A16/.

Houser, J.N., D.L. Bade, J.J. Cole, and M.L. Pace. 2003. "The Dual Influences of Dissolved Organic Carbon on Hypolimnetic Metabolism: Organic Substrate and Photosynthetic Reduction." *Biogeochemistry* 64 (2): 247–69. https://doi.org/10.1023/A:1024933931691.

Hunt, R.J. 2006. "Ground Water Modeling Applications Using the Analytic Element Method." *Groundwater* 44 (1): 5–15. https://doi.org/10.1111/j.1745-6584.2005.00143.x.

Hunt, R.J., M.P. Anderson, and V.A. Kelson. 1998. "Improving a Complex Finite-Difference Ground Water Flow Model through the Use of an Analytic Element Screening Model." *Groundwater* 36 (6): 1011–17. https://doi.org/10.1111/j.1745-6584.1998.tb02108.x.

Hunt, R.J., D.T. Feinstein, C.D. Pint, and M.P. Anderson. 2006. "The Importance of Diverse Data Types to Calibrate a Watershed Model of the Trout Lake Basin, Northern Wisconsin, USA." *Journal of Hydrology* 321 (1–4): 286–96. https://doi.org/10.1016/j.jhydrol.2005.08.005.

Hunt, R.J., J.F. Walker, W.R. Selbig, S.M. Westenbroek, and R.S. Regan. 2013. "Simulation of Climate-Change Effects on Streamflow, Lake Water Budgets, and Stream Temperature Using GSFLOW and SNTEMP, Trout Lake Watershed, Wisconsin." *U.S. Geological Survey Scientific Investigations Report 2013-5159*. https://pubs.usgs.gov/sir/2013/5159/.

Jones, S.E., R.J. Newton, and K.D. McMahon. 2009. "Evidence for Structuring of Bacterial Community Composition by Organic Carbon Source in Temperate Lakes." *Environmental Microbiology* 11 (9): 2463–72. https://doi.org/10.1111/j.1462-2920.2009.01977.x.

Jones, S.E., J.A. Zwart, P.T. Kelly, and C.T. Solomon. 2018. "Hydrologic Setting Constrains Lake Heterotrophy and Terrestrial Carbon Fate." *Limnology and Oceanography Letters* 3 (3): 256–64. https://doi.org/10.1002/lol2.10054.

Kluge, T., J. Ilmberger, C. Von Rohden, and W. Aeschbach-Hertig. 2007. "Tracing and Quantifying Groundwater Inflow into Lakes Using Radon-222." *Hydrology and Earth System Sciences Discussions* 4 (3): 1519–48.

Kollet, S.J., and R.M. Maxwell. 2006. "Integrated Surface-Groundwater Flow Modeling: A Free-Surface Overland Flow Boundary Condition in a Parallel Groundwater Flow Model." *Advances in Water Resources* 29 (7): 945–58. https://doi.org/10.1016/j.advwatres.2005.08.006.

Kollet, S.J., and R.M. Maxwell. 2008. "Capturing the Influence of Groundwater Dynamics on Land Surface Processes Using an Integrated, Distributed Watershed Model." *Water Resources Research* 44 (2). https://doi.org/10.1029/2007WR006004.

Leavesley, G.H., R.W. Lichty, B.M. Troutman, and L.G. Saindon. 1983. "Precipitation-Runoff Modeling System User's Manual." *U.S. Geological Survey Water-Resources Investigations Report 83-4238*. https://pubs.er.usgs.gov/publication/wri834238.

Lenters, J.D., T.K. Kratz, and C.J. Bowser. 2005. "Effects of Climate Variability on Lake Evaporation: Results from a Long-Term Energy Budget Study of Sparkling Lake, Northern Wisconsin (USA)." *Journal of Hydrology* 308 (1–4): 168–95. https://doi.org/10.1016/j.jhydrol.2004.10.028.

Liang, X., D.P. Lettenmaier, E.F. Wood, and S.J. Burges. 1994. "A Simple Hydrologically Based Model of Land Surface Water and Energy Fluxes for General Circulation Models." *Journal of Geophysical Research: Atmospheres* 99 (D7): 14415–28. https://doi.org/10.1029/94JD00483.

Liang, X., E.F. Wood, and D.P. Lettenmaier. 1996. "Surface Soil Moisture Parameterization of the VIC-2L Model: Evaluation and Modifications." *Global and Planetary Change* 13: 195–206. https://doi.org/10.1016/0921-8181(95)00046-1.

Lillie, R.A., and J.W. Mason. 1983. "Limnological Characteristics of Wisconsin Lakes." *Department of Natural Resources Technical Bulletin No. 138*. https://dnr.wi.gov/files/PDF/pubs/ss/ss0138.pdf.

Livneh, B., T.J. Bohn, D.W. Pierce, F. Munoz-Arriola, B. Nijssen, R. Vose, and L. Brekke. 2015. "A Spatially Comprehensive, Hydrometeorological Data Set for Mexico, the US, and Southern Canada 1950–2013." *Scientific Data* 2: 150042. https://doi.org/10.1038/sdata.2015.42 (2015).

Livneh, B., E.A. Rosenberg, C. Lin, B. Nijssen, V. Mishra, K.M. Andreadis, and D.P. Lettenmaier. 2013. "A Long-Term Hydrologically Based Dataset of Land Surface Fluxes and States for the Conterminous United States: Update and Extensions." *Journal of Climate* 26 (23): 9384–92. https://doi.org/10.1175/JCLI-D-12-00508.1.

Lohmann, D., R. Nolte-Holube, and E. Raschke. 1996. "A Large-Scale Horizontal Routing Model to Be Coupled to Land Surface Parametrization Schemes." *Tellus* 48A: 708–21. https://doi.org/10.1034/j.1600-0870.1996.t01-3-00009.x.

Magee, M.R., C.H. Wu, D.M. Robertson, R.C. Lathrop, and D.P. Hamilton. 2016. "Trends and Abrupt Changes in 104 Years of Ice Cover and Water Temperature in a Dimictic Lake in Response to Air Temperature, Wind Speed, and Water Clarity Drivers." *Hydrology and Earth System Sciences* 20 (5): 1681. https://doi.org/10.5194/hess-20-1681-2016.

Magnuson, J.J., T.K. Kratz, and B.J. Benson, eds. 2006. *Long-Term Dynamics of Lakes in the Landscape: Long-Term Ecological Research on North Temperate Lakes*. Oxford, United Kingdom: Oxford University Press on Demand.

Markstrom, S.L., R.G. Niswonger, R.S. Regan, D.E. Prudic, and P.M. Barlow. 2008. "GSFLOW — Coupled Ground-Water and Surface-Water Flow Model Based on the Integration of the Precipitation-Runoff Modeling System (PRMS) and the Modular Ground-Water Flow Model (MODFLOW-2005)." *U.S. Geological Survey Techniques and Methods 6-D1*. https://pubs.er.usgs.gov/publication/tm6D1.

Maurer, E.P., A.W. Wood, J.C. Adam, D.P. Lettenmaier, and B. Nijssen. 2002. "A Long-Term Hydrologically Based Dataset of Land Surface Fluxes and States for the Conterminous United States." *Journal of Climate* 15 (22): 3237–51. https://doi.org/10.1175/1520-0442(2002) 015<3237:ALTHBD>2.0.CO;2.

McDonald, M.G., and A.W. Harbaugh. 1984. "A Modular Three-Dimensional Finite-Difference Ground-Water Flow Model." *U.S. Geological Survey Open-File Report 83–875*. https://pubs.er.usgs.gov/publication/ofr83875.

Merritt, M.L., and L.F. Konikow. 2000. "Documentation of a Computer Program to Simulate Lake-Aquifer Interaction Using the MODFLOW Ground-Water Flow Model and the MOC3D Solute-Transport Model." *U.S. Geological Survey Water-Resources Investigations Report 2000–4167*. https://pubs.er.usgs.gov/publication/wri004167.

Messager, M.L., B. Lehner, G. Grill, I. Nedeva, and O. Schmitt. 2016. "Estimating the Volume and Age of Water Stored in Global Lakes Using a Geo-Statistical Approach." *Nature Communications* 7: 13603. https://doi.org/10.1038/ncomms13603 (2016).

Mitchell, K., P. Houser, E. Wood, J. Schaake, D. Tarpley, D. Lettenmaier, W. Higgins, C. Marshall, D. Lohmann, M. Ek, and B. Cosgrove. 1999. "GCIP Land Data Assimilation System (LDAS) Project Now Underway." *Gewex News* 9 (4): 3–6.

Muffels, C.T. 2008. "Application of the LSQR Algorithm to the Calibration of a Regional Groundwater Flow Model — Trout Lake Basin, Vilas County, Wisconsin." MS thesis, University of Wisconsin–Madison.

Niu, J., C. Shen, S.G. Li, and M.S. Phanikumar. 2014. "Quantifying Storage Changes in Regional Great Lakes Watersheds Using a Coupled Subsurface-Land Surface Process Model and GRACE, MODIS Products." *Water Resources Research* 50 (9): 7359–77. https://doi.org/10.1002/2014WR015589.

Oliver, S.K., P.A. Soranno, C.E. Fergus, T. Wagner, L.A. Winslow, C.E. Scott, and E.H. Stanley. 2016. "Prediction of Lake Depth Across a 17-State Region in the United States." *Inland Waters* 6 (3): 314–24. https://doi.org/10.1080/IW-6.3.957.

Peterson, G.D., T.D. Beard, Jr., B.E. Beisner, E.M. Bennett, S.R. Carpenter, G.S. Cumming, and T.D. Havlicek. 2003. "Assessing Future Ecosystem Services: A Case Study of the Northern Highlands Lake District, Wisconsin." *Conservation Ecology* 7 (3): 1.

Pint, C.D. 2002. "A Groundwater Flow Model of the Trout Lake Basin, Wisconsin — Calibration and Lake Capture Zone Analysis." MS thesis, University of Wisconsin–Madison.

Qu, Y., and C.J. Duffy. 2007. "A Semidiscrete Finite Volume Formulation for Multiprocess Watershed Simulation." *Water Resources Research* 43 (8). https://doi.org/10.1029/2006WR005752.

Read, E.K., V.P. Patil, S.K. Oliver, A.L. Hetherington, J.A. Brentrup, J.A. Zwart, and H.A. Dugan. 2015. "The Importance of Lake-Specific Characteristics for Water Quality Across the Continental United States." *Ecological Applications* 25 (4): 943–55. https://doi.org/10.1890/14-0935.1.

Shen, C., and M.S. Phanikumar. 2010. "A Process-Based, Distributed Hydrologic Model Based on a Large-Scale Method for Surface–Subsurface Coupling." *Advances in Water Resources* 33 (12): 1524–41. https://doi.org/10.1016/j.advwatres.2010.09.002.

Soranno, P.A., E.G. Bissell, K.S. Cheruvelil, S.T. Christel, S.M. Collins, C.E. Fergus, C.T. Filstrup, J.F. Lapierre, N.R. Lottig, S.K. Oliver, and C.E. Scott. 2015. "Building a Multi-Scaled Geospatial Temporal Ecology Database from Disparate Data Sources: Fostering Open Science and Data Reuse." *GigaScience* 4 (1): 28. https://doi.org/10.1186/s13742-015-0067-4.

Strack, O.D. 1989. *Groundwater Mechanics*. Englewood Cliffs, NJ: Prentice Hall.

Strack, O.D. 2003. "Theory and Applications of the Analytic Element Method." *Reviews of Geophysics* 41 (2): https://doi.org/10.1029/2002RG000111.

Striegl, R.G., J.E. Schindler, K.P. Wickland, D.C. Hudson, and G.C. Knight. 2000. "Patterns of Carbon Dioxide and Methane Saturation in 34 Minnesota and Wisconsin Lakes." *Internationale Vereinigung fur Theoretische und Angewandte Limnologie Verhandlungen* 27 (3): 1424–27. https://doi.org/10.1080/03680770.1998.11901471.

Torak, L.J. 1993. "A Modular Finite-Element Model (MODFE) for Areal and Axisymmetric Ground-Water-Flow Problems, Part 1: Model Description and User's Manual." *U.S. Geological Survey, Techniques of Water-Resources Investigations, Book 6, Chapter A3*. https://pubs.er.usgs.gov/publication/twri06A3.

Trescott, P.C. 1975. "Documentation of Finite-Difference Model for Simulation of Three-Dimensional Ground-Water Flow." *U.S. Geological Survey Open-File Report 75–438*. https://pubs.er.usgs.gov/publication/ofr75438.

Vachon, D., and P.A. del Giorgio. 2014. "Whole-Lake CO_2 Dynamics in Response to Storm Events in Two Morphologically Different Lakes." *Ecosystems* 17: 1338–53. https://doi.org/10.1007/s10021-014-9799-8.

Vachon, D., Y.T. Prairie, F. Guillemette, and P.A. del Giorgio. 2017. "Modeling Allochthonous Dissolved Organic Carbon Mineralization Under Variable Hydrologic Regimes in Boreal Lakes." *Ecosystems* 20 (4): 781–95. https://doi.org/10.1007/s10021-016-0057-0.

Wetzel, R.G. 2001. *Limnology: Lake and River Ecosystems*. Oxford, United Kingdom: Gulf Professional Publishing.

Winter, T.C. 1999. "Relation of Streams, Lakes, and Wetlands to Groundwater Flow Systems." *Hydrogeology Journal* 7 (1): 28–45. https://doi.org/10.1007/s100400050178.

Zhang, T., P.A. Soranno, K.S. Cheruvelil, D.B. Kramer, M.T. Bremigan, and A. Ligmann-Zielinska. 2012. "Evaluating the Effects of Upstream Lakes and Wetlands on Lake Phosphorus Concentrations Using a Spatially-Explicit Model." *Landscape Ecology* 27 (7): 1015–30. https://doi.org/10.1007/s10980-012-9762-z.

Zwart, J.A., Z.J. Hanson, J. Vanderwall, D. Bolster, A. Hamlet, and S.E. Jones. 2018. "Spatially Explicit, Regional-Scale Simulation of Lake Carbon Fluxes." *Global Biogeochemical Cycles*. https://doi.org/10.1002/2017GB005843.

Zwart, J.A., S.D. Sebestyen, C.T. Solomon, and S.E. Jones. 2017. "The Influence of Hydrologic Residence Time on Lake Carbon Cycling Dynamics Following Extreme Precipitation Events." *Ecosystems* 20 (5): 1000–14. https://doi.org/10.1007/s10021-016-0088-6.